Three-dimensional models of cochlear implants: a review of their development and how they could support management and maintenance of cochlear implant performance

Tania Hanekom & Johan J Hanekom

Bioengineering, University of Pretoria, South Africa

Running title: 3D modelling of cochlear implants

Abstract

Three-dimensional (3D) computational modelling of the auditory periphery forms an integral part of modern-day research in cochlear implants (CIs). These models consist of a volume conduction description of implanted stimulation electrodes and the current distribution around these, coupled to auditory nerve fibre models. Cochlear neural activation patterns can then be predicted for a given input stimulus. The objective of this article is to present the context of 3D modelling within the field of CIs, the different models and approaches to models that have been developed over the years, as well as the applications and potential applications of these models. The process of development of 3D models is discussed, and the article places specific emphasis on the complementary roles of generic models and user-specific models, as the latter is important for translation of these models into clinical application.

Keywords: 3D cochlear modelling, User-specific models, Volume conduction model, Neural model

Introduction

An understanding of the role that the electro-anatomy of the cochlea plays in hearing has already been recognised by Georg von Békésy in 1951. His article on the electroanatomy of the cochlea (von Békésy 1951) begins with the following profound statement: "For a thorough understanding of the cochlear microphonics it is necessary to investigate the electrical geometry of the cochlea, because only with a knowledge of the voltages and the

resistance patterns can we construct an over-all picture of the electrical situation in the cochlea". This statement still holds true after 65 years of research on auditory perception. While much progress has been made in the development of our understanding of the electro-anatomy of the cochlea since von Békésy's rudimentary lumped-parameter description thereof, there is still a vast number of unknowns that need to be captured in the intricacies of our contemporary computational models of the auditory system.

Three-dimensional (3D) computational modelling of the auditory periphery forms an integral part of modern-day research in cochlear implants (CIs). 3D CI models refer to models that include spatial dimensionality in the description of the functioning of the cochlea. These models provide a description of either the micromechanical characteristics of the cochlea, or of the electrophysiological behaviour of the system. This review focuses on 3D electro-anatomical models of the auditory system that facilitate prediction of electrophysiological behaviour of the electrically stimulated cochlea.

3D CI models provide a simulated invasive view of the cochlear electro- and neurophysiology that facilitates a depth and scale of investigation that is not generally feasible in animal models and especially not in live human users. The objective of this article is to present the context of 3D modelling within the field of CIs, the different models and approaches to models that have been developed over the years, as well as the applications and potential applications of these models. The article also places specific emphasis on the complementary roles of generic and user-specific models, as the latter is important for translation of these models into the clinical domain.

The cochlear implant has been established as the treatment of choice for severe to profound sensorineural deafness. Numbers of implant users reported in literature (Community 2008; De Quesada 1995; Disorders 2011; 2014; Jeschke et al. 2015; National Institute on Deafness and Other Communication Disorders 2014; Nussbaum et al. 2002;

Peters et al. 2010; Samp 2010; Zaidman-Zait 2010) show an exponential increase from around 5000 users in 1990 to more than 300 000 users worldwide in 2015, which is indicative of the exceptional success and general acceptance of the device. Speech understanding in quiet has steadily increased with the developing technology until the early 2000s, but has stabilised at around 80% on average (Zeng et al. 2008). However, in spite of the success of the device, hearing performance varies greatly among individuals (Sladen et al. 2015). The benefit range of CIs starts at basic rhythm perception with very poor to no tonal content at the low end of performance, good speech perception in quiet and a considerable appreciation for music (Maarefvand et al. 2013) at the high end of performance. Speech perception in noise and music perception are generally quite poor for the average cochlear implant user, with a decrease in performance between quiet and +15 dB SNR of around 25% (Sladen et al. 2015) and around 25% melody recognition (Drennan et al. 2015) respectively. The variation in perceptual outcomes among CI users may be caused by a myriad of factors that include (i) peripheral factors such as intracochlear electrode location (Finley et al. 2008; Rebscher et al. 2007), cochlear morphology (Frijns et al. 2001; Malherbe et al. 2013; 2015a), neural survival profiles(Blamey et al. 1996; Gantz et al. 1993; Hassanzadeh et al. 2002; Won et al. 2015) and insertion trauma (Adunka et al. 2006; Briaire et al. 2006; Verbist et al. 2009), and (ii) central processing aspects such as variations in the neural pathways and accompanying processing (Isaiah et al. 2014; Vermeire et al. 2015).

Since the primary objective of CI research is to inform the development of CI technology to the extent where technology may provide normal hearing to all severe to profound hearing impaired individuals, the variation in user outcomes is a major area of investigation. User variation in performance is a manifestation of the inherent characteristics of the individual auditory system that govern its behaviour in response to electrical stimulation. Many of the factors that affect user performance are not well-understood,

clouding the optimisation process that must result in the seamless biophysical interface between technology and biology. Ultimately, research in CI thus aims to:

(i) produce an exhaustive understanding of the electro- and neurophysiology of the human auditory system to allow researchers to develop a comprehensive understanding of how biological structures and processes produce the neural output that is observed through electrophysiological measurements from the auditory nerve;

(ii) produce a comprehensive understanding of the entire processing pathway of sound from the auditory periphery to perception;

(iii) optimize information transfer to the brain exploiting neuroplasticity for information decoding;

(iv) apply knowledge of neural excitation and auditory processing to direct the design of CI technology so that this may exploit the characteristics of the auditory system in such a way that the interface is generally seamless and undetected by the human auditory system;

(v) personalise cochlear implant technology to provide an optimised interface with a specific user's auditory system.

Clarity on many of the factors that produce user variability could conceivably be more readily obtained if the specific system were accessible to invasive, in vivo experimental and quantification procedures to determine precise electro- and neurophysiological functioning in response to applied electrical stimuli. However, while these procedures may be a viable investigative option in animal models, they are for obvious reasons not suited to probe the auditory system of live CI users. Research into the functioning of CIs in humans must therefore rely on techniques and procedures that are based on psychophysical, neurophysiological and medical imaging data that may be collected non-invasively.

A systematic integration of existing and new knowledge of the functioning of the auditory system is required to give purpose and direction to research in user-variability. By implication, available information needs to be fused to provide a detailed, multi-faceted description of the auditory system under electrical stimulation conditions. One of the ways in which structure, function and data can be fused is through a model description of a user's auditory system. This review elaborates on the toolbase that 3D computational models of CIs provide to address the four aspects of CI research as presented above. In the following sections we first review the approach to constructing 3D models and then the various 3D models that have been developed over the years. We then consider application of 3D models in research and the translation of these models to the clinical domain and finally provide a perspective on the future of 3D models in CI research.

Creation of 3D volumetric descriptions of the auditory periphery

Initial attempts at a 3D description of the electro-anatomy of the cochlea were limited by the manual nature of computations until the 1980s, when personal computers became available.. Early models were lumped-parameter models that described the unrolled intra-scalar structure of the cochlea, i.e. ignoring the spiralling nature of the inner ear, using active and passive components (Cannon 1976; Johnstone et al. 1966; Strelioff 1973a; von Békésy 1951). However, to preserve the 3D geometric fidelity of the cochlea, a volume conduction (VC) description is required. For the past 15 years, VC models have been integrated with auditory nerve fibre (ANF) models to interpret the predicted potential distributions in terms of neuro-electrophysiological behaviour that may eventually be linked to perception. A later section will briefly consider integration of neural models with VC models of the cochlea.

3D modelling in CI has mainly been directed at the biophysical interface between the auditory periphery (i.e., cochlea and peripheral auditory nerve fibres that innervate the cochlea) and the implant technology. The biophysical interface is a complex interaction

between the CI technology and the cochlear environment, and is characterised, among others, by the anatomical morphology of the cochlea, the electrical characteristics of cochlear tissues, the distribution and trajectories of neurons and their degeneration profiles, the design of the electrode array and its final intra-scalar location, and lesions as a result of insertion damage. This section will briefly interpret the five steps in a typical model generation workflow (MGW) to create a 3D VC model of the cochlea, namely (1) imaging of the cochlea, (2) geometric assessment, (3) refinement (interpolation, extrapolation and image registration), (4) model structure generation, and (5) physics setup and solving of the model.

Imaging the cochlea

The first step in the model generation workflow (MGW) is imaging of the cochlea. The better the imaging resolution, the more accurately the structure of the cochlea can be reconstructed. Various techniques are available to image morphologic characteristics, and these can be divided into imaging techniques that are suitable for animal or cadaveric materials and techniques that are suited to image live animal subjects or human users. The major distinction between the two types of imaging techniques is the resolution of the image data: the first type of technique currently provides higher resolution images in general than those provided by imaging that may be applied to visualise living cochleae since these make use of methods that are either detrimental to live tissue or destructive in nature. Figure 1 illustrates the potential range of image resolutions among different imaging modalities. The highly-detailed image in Figure 1a as well as the lower-resolution micro-computed tomography (μCT) image shown in Figure 1b are only obtainable for non-living cochleae, while the conventional spiral-CT image shown in Figure 1c may be obtained for live cochleae. For this reason, steps 2 and 3 of the MGW are directly affected by the imaging technique. A further implication is that imaging techniques applicable to non-living cochleae are better suited to the creation of generalised or exploratory user-specific models, while

techniques suitable to image live cochleae provide the source data for user-specific models that may be clinically applied.

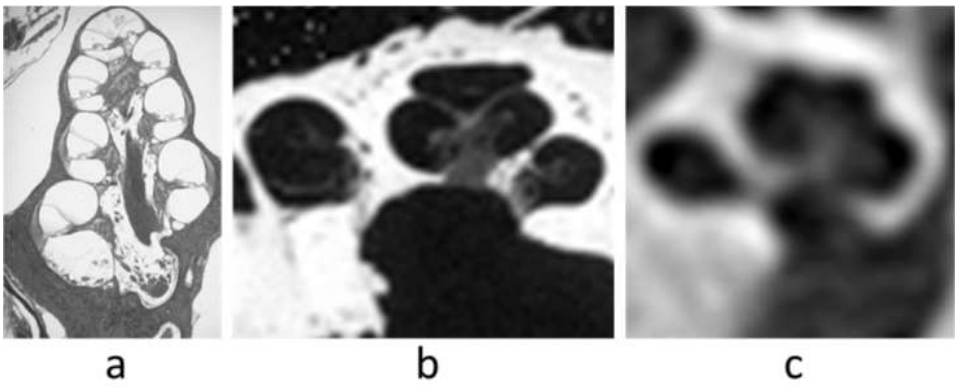

Figure 1. Images produced for mid-modiolar sections through the cochlea demonstrating image resolution. Sectional imaging in the form of a photomicrograph of a histologic section through a guinea pig cochlea[1] revealing delicate details of the internal structures of the organ (a), radiation-based μCT image of a human temporal bone showing limited detail about the internal structures of the cochlea (b), and clinically obtained spiral-CT image demonstrating poor resolution and no delineation of internal structures (c).

The choice of which imaging modality should be selected to provide the source data for a 3D cochlear model ultimately depends on three factors: whether the cochlea is alive or non-living, the type of detail that is required and the type of technology that is available to the research team. While radiation-based imaging methods (e.g. the various computed tomography techniques) are non-destructive, they generally cannot delineate soft tissue structures such as the basilar membrane or scala media structures, though the spiral lamina is generally well-demonstrated. If visible, the location of the spiral lamina may provide some indication of the internal structure of the cochlea. Sectioning-based techniques need to be employed if micro-details of the cochlear structures are required, such as the high-resolution models presented by Tran et al. (2014) and Wong et al. (2016), but none of these techniques

[1] Reproduced with permission.

http://ocw.tufts.edu/Content/72/imagegallery/1362321/1369037/1378580

are suitable for imaging live cochleae. However, sectioning-based images, such as photomicrographs of histologic sections, may prove valuable to augment lower-resolution CT delineation of the bony boundaries of the cochlea with high resolution detail of the inner structures of the cochlea (Malherbe et al. 2013; 2015a).

Imaging techniques that have been used as source data to create models of non-living human and animal cochleae include physical sectioning techniques such as histologic sectioning (Liu et al. 2007; Wada et al. 1998; Zhang et al. 2011; Zhaol et al. 2007), micro-grinding imaging (Rau et al. 2011) and serial sectioning (Tran et al. 2014), optical sectioning such as orthogonal-plane fluorescence optical sectioning (OPFOS) (Voie et al. 1995) and radiation-based μCT (Lee et al. 2010; Malherbe et al. 2013; Poznyakovskiy et al. 2008). The resolution of physical sectioning techniques is usually the poorest in the direction of abrasion (i.e. perpendicular to the plane of imaging) because of the finite thickness with which material may be removed to reveal a subsequent section. The details of the section are captured by photographic means of which the resolution is limited by the objective and the resolution of the charge-coupled device (CCD) sensor of the particular camera. The photographic resolution is usually much higher than the slice thickness of the abrasion process which may provide superior image quality from which the details of the delicate inner structures of the cochlea may be discerned and digitised to micrometre accuracy. A slice thickness of 100 μm has been reported for micro-grinding imaging (Rau et al. 2011) while serial sectioning can achieve slice thicknesses of 0.33 mm to 1 mm (Tran et al. 2014). OPFOS, an optical sectioning technique and μCT that is a radiation-based technique have been reported to provide a resolution of around 10 to 30 μm pixel size (Le Breton et al. 2015; Malherbe et al. 2013; Voie et al. 1993) within the context of cochlear imaging.

Imaging modalities that are safe to use post-operatively on living cochleae are mainly spiral or cone-beam computed tomography (CT) and in some cases x-rays that are taken to

facilitate epipolar stereophotogrammetry (Yoo et al. 2004). Cochlear structures that are important to represent in a 3D model and that can be delineated with spiral-CT include the bony labyrinth, osseous spiral lamina (sometimes) and modiolus (Martinez-Monedero et al. 2011). The integrity of the model may be validated by CT measures such as cochlear size variability (Pelliccia et al. 2014), cochlear length (Connor et al. 2009; Escudé et al. 2006; Krombach et al. 2005; Martinez-Monedero et al. 2011), mean vertical diameter (Escudé et al. 2006; Martinez-Monedero et al. 2011), total cochlear height (Krombach et al. 2005) and height of the basal turn (Krombach et al. 2005), and quantified data are available in the literature for all of these. Electrode position, which is a key parameter in user-specific models, is also assessable through CT (Escudé et al. 2006; Ketten et al. 1998a; Skinner et al. 2002; van der Marel et al. 2014; van Wermeskerken et al. 2007; Verbist et al. 2010a; Verbist et al. 2010b). In addition, cone-beam CT (CBCT) is becoming commonly available in a clinical setting and has been used to assess cochlear length (Wurfel et al. 2014) and electrode location (Zou et al. 2015). CBCT also provides a significantly lower radiation dose and increased spatial relationship when compared to spiral-CT (Vaid et al. 2014).

As well, magnetic resonance imaging (MRI) may be applied pre-operatively to quantify the geometric characteristics of the fluid-filled spaces in the cochlea for co-registration with post-operative CT data in an attempt to increase the level of detail in the 3D description of the cochlear structures. MRI can be used to determine modiolar area and volume (Kendi et al. 2004; Naganawa et al. 1999), volume of the labyrinth (Kendi et al. 2004; Melhem et al. 1998; Neri et al. 2000), cochlear nerve preservation (Ketten et al. 1998b; Lane et al. 2007) and length of the cochlea (Sobrinho et al. 2009), which are all parameters that may either be incorporated into the 3D geometry or used to validate the integrity of a model representation of a cochlea. MRI is specifically used for evaluating luminal ossification and inner ear patency before cochlear implantation (Chaturvedi et al. 2006;

Fishman 2012; Murugasu et al. 1999; Seitz et al. 2001; Taha et al. 2015; Vaid et al. 2014) which are important factors to consider when developing user-specific models.

Geometric assessment

The first important set of geometric assessment tools is image post-processing to enhance the features in the image that are important to describe the geometry. These include deblurring algorithms to enhance delineation of anatomical features and implant electrode positions in the cochlea (Wang et al. 1998).

Once an image or image stack of the cochlea has been obtained, the next phase in the development of 3D computational models is capturing of geometric parameters from the image data. The first consideration in 3D image data is to orient the visual representation of the data relative to the geometry of the cochlea. The preferred view for digitisation of geometric parameters to construct cochlear models is a mid-modiolar view that is derived by reconstructing the image data using the cochlear view (Verbist et al. 2010b). This view allows visualisation of the different cochlear canals. By reslicing the reconstructed image data at fixed degree intervals around an axis directed through the centre of the modiolus, the geometric characteristics of the structure may be determined.

Landmark assessment is frequently used to register coordinates for model generation. An anatomical landmark is a meaningful point that ensures correspondence within measurements of a structure. Identification of landmarks is a time-consuming process that requires considerable anatomical understanding (Bookstein 1997) and is usually a manual process. Examples of anatomical landmarks in cochleae that are relevant to the construction of 3D models are the lateral-most point on the cochlear wall, the lateral-most and medial-most points of the spiral lamina and the points that define the cochlear inlet. Using a midmodiolar approach to visualise the image data, a specific landmark would be followed along its spiral trajectory and its coordinates registered around the reconstructed image stack.

Segmentation is an alternative procedure that involves the identification of different anatomical structures that make up the cochlea by means of selection of the structures either manually by an experienced investigator (Seemann et al. 1999), semi-automatically with the aid of software packages such as Amira[2] (Wang et al. 2006) or ScanIP (Tran et al. 2014) or fully automatically through the use of sophisticated software (Noble et al. 2011; Reda et al. 2014). Semi-automatic or automatic segmentation methods usually rely on the colour or grayscale value of a pixel that is associated with a specific structure or tissue. Experience with the anatomy of the structure that is segmented is again important to set up the correct parameters for segmentation procedures.

The trajectory of the electrode array may be determined either by landmarking or by segmentation processes as described for delineation of the cochlear structures. This may, however, be complicated by metal artefacts that are produced in CT images and cause oversaturation of the image in the vicinity of the electrode contacts (Skinner et al. 1994). The exact location of extra-cochlear return electrodes may additionally be determined from imaging data for inclusion in 3D models (Malherbe et al. 2015b).

Refinement: interpolation, extrapolation and image registration

The type of procedure that was used to assess the geometry will determine how much data refinement is required. Images with high resolution and clearly discernible tissue boundaries may be suitable for automatic segmentation and subsequent automatic model generation, thereby rendering the refinement step in the MGW redundant. This approach has indeed been tested, but it tends to allow a restricted description of the inner structures of the

[2] 3D software platform for visualizing, manipulating, and understanding biological image data. http://www.fei.com/software/amira-3d-for-life-sciences/

cochlea, e.g. the cochlea would be rendered as one fluid-filled cavity or at most be resolved into separate descriptions of the scala tympani and scala vestibuli (Noble et al. 2011).

However, to generate models with a high level of detail, researchers must typically resort to semi-automatic (Tran et al. 2014) or manual methods (Malherbe et al. 2015a). The raw data obtained in this manner are frequently not suitable to translate into a 3D model structure because of noise introduced by the geometric assessment method. For example, in landmark assessment as employed by Malherbe et al. (2015a), the representation of points on structures parallel to the modiolar axis tend to be noisy in the direction parallel to the axis, while it may be more accurately assessed in a direction perpendicular to the axis simply because it is easier to place a point on the transition of the boundary than on a line along the boundary. This concept is illustrated in Figure 2 that demonstrates the ambiguity in one of the dimensions of measurement.

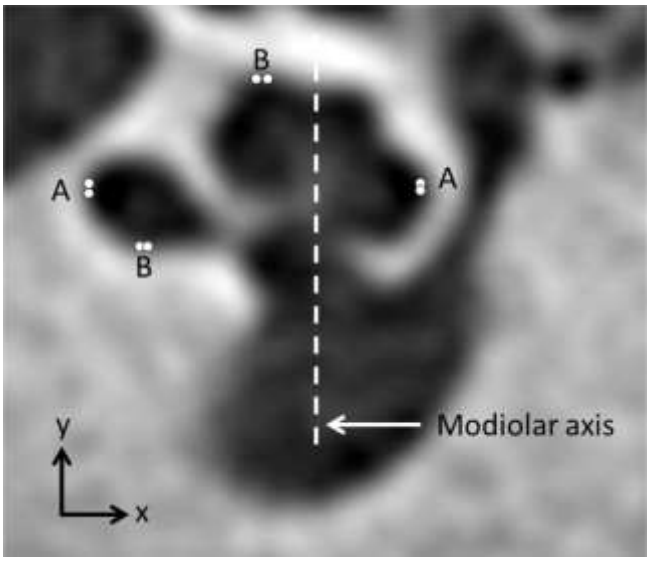

Figure 2. Landmarks parallel to the modiolar axis are easier to resolve in the direction of the x-axis (A), i.e. their y-axis representation tend to be noisy, while landmarks parallel to the x-axis are easier to resolve in the y-direction (B) with a noisier assessment of their x-axis representation.

To use these data effectively, pre-processing is required to mitigate the effect of measurement errors by smoothing out the boundaries and in this way also simplify reading and reconstructing geometries from the input values to the 3D modelling software. One pre-processing approach is curve fitting on a set of measurements that describe the trajectory of a specific landmark along the cochlear spiral. Approaches that have been followed include a helicospiral approximation method that fits a circular representation of the combined area of the scala tympani and scala vestibuli to a helicospiral model (Yoo et al. 2000b), interpolation of the data through third order cubic splines (Malherbe et al. 2013), and the use of a procrustes (scaling, translating and mirroring) approach to fit measured landmarks to cochlear spirals obtained from literature (Malherbe et al. 2015a). The level of accuracy that may be achieved through curve fitting methods depends on the number of data points that describe the landmark. A single mid-modiolar section was used to create the guinea pig model of Malherbe et al. (2013) and the cat model of Kang et al. (2015) by fitting spirals through the landmarks measured on this image. However, additional sections had to be measured at the base of the cochlea since the spiral description of this area was insufficient as a result of local irregularities in shape. An improved description of the characteristics of the spiral may be obtained by employing more data points to describe the trajectory of the landmark (Malherbe et al. 2015a) or by using data that was obtained through segmentation methods on a high-resolution image stack (Wong et al. 2016).

Image registration, i.e. the process of transforming different sets of geometric data into one coordinate system, is also widely used to improve the level of detail in models. This technique is particularly appropriate when the main geometric data source has low resolution. Examples where this approach was followed abound, for instance 3D localisation of individual cochlear implant electrodes by the use of two X-ray images registered with a spiral computed tomography technique (Yoo et al. 2004), description of inner structure details by

registration of μCT or CT data with templates of the cochlear structures that were derived from high-resolution images of histologic sections (Malherbe et al. 2013; 2015a), and a method that uses a semi-automatic technique to create 3D models of the guinea pig cochlea by registration of μCT and histological images (Lee et al. 2010).

Identification of the electrode array trajectory for inclusion into user-specific models also requires data refinement as CT and X-ray imaging are the only options available for live cochleae and, as mentioned, metal artefacts produce significant overexposure on these images. Most approaches to estimate the position of the electrode array relies on intensity thresholding to localise the voxels with the highest numerical values which indicate the locations of the electrodes (Malherbe et al. 2013; Teymouri et al. 2011).

Model structure generation

Model construction involves the creation of 3D geometric entities based on the processed anatomical measurement data. Various techniques have been developed for 3D model generation of the cochlea. The first VC model of the cochlea developed by Girzon (1987) simply sampled the geometry on a fixed grid with a maximum of 512 x 512 x 37 elements throughout the cochlear volume. The grid size, and therefore the resolution of the model, was mainly limited by the computational effort that the numerical method that was used required.

Extrusion of a template description of a section through one turn of the cochlea followed the initial grid sampling approach (Finley et al. 1990) and is one of the simplest methods that can be used to prepare geometries for volume and boundary based numerical methods such as the finite element (FE) and boundary element (BE) methods. Extrusion has been and is still being applied to generate rotationally symmetric models (Frijns et al. 1996) and spiralling models (Briaire et al. 2000b; Hanekom 2001; Kang et al. 2015) of the cochlea.

A related technique is to place a simplified representation of the cross section of the scalae perpendicular to a spiral that follows a central path through the ducts. This is relatively uncomplicated to set up with modern software if the relevant geometric parameters are available. The resulting framework is then converted into a meshed polygon description of the cochlea (Yoo et al. 2000a).

Semi-automatic to automatic segmentation through region growing processing is a method that is widely used to visualise cochlear structures (Rodt et al. 2002; Seemann et al. 1999). It creates volumes by merging neighbouring pixels that satisfy a homogeneity criterion. Any 2D image stack that provides differentiation among the structures of interest through intensity or colour variation may be subjected to this type of processing. This method has been employed to create VC models of the cochlea, but typically requires an increased amount of manual intervention with an increased need for detail (Tran et al. 2014; Wong et al. 2016). Surface face models that can be imported in modelling software packages by conversion into, for example, an STL file format may then be created from the volumes that result from this process. The general approach is supported by a wide variety of dedicated 3D software such as Amira (Li et al. 2007) or ScanIP (Tran et al. 2014), or through the use of a workflow that prepares the segmentation data through custom code and then uses 3D rendering software to create the volumes (Rau et al. 2011).

Landmarking provides an alternative approach to region growing processing to develop the model structure. General technical computing software such as Matlab[3] can be used to interpret geometry from the refined landmark data generated in the third MGW step. Anatomical structures are delineated by creating a wire framework from the landmarks that describe them. The framework is used to creating surfaces that outline each structure. These

[3] Technical computing language. http://www.mathworks.com/

are then described in a format that can be interpreted by finite element modelling software such as Comsol[4] (Malherbe et al. 2013).

The electrode array may either be reconstructed using the same approach as followed for reconstruction of the cochlear anatomy, or modelling can be based on the known dimensions of the array as provided by the manufacturer and then inserted into the cochlear model using a registration process (Kalkman et al. 2015; Tran et al. 2014).

Physics setup and solving of the model

Tissue impedance characteristics

After the geometry of the model has been created, the electrical characteristics for tissues need to be assigned. In an electrically stimulated cochlea, current flows from a stimulating electrode to a return electrode via the cochlear tissues. The shape and resistivities of these tissues determine the path that current will follow (Micco et al. 2006). Obtaining an accurate geometric representation of cochlear structures will not result in more accurate predictions of current patterns if the resistivities assigned to those structures are not accurately represented in the model.

Traditionally, tissue impedances are implemented as pure resistances based on the observation by Spelman et al. (1982) that minimal phase lag occur in cochlear tissues up to 12.5 kHz. A basic set of tissue resistivities that are used in 3D VC models has been reported in numerous studies (Frijns et al. 1996; Hanekom 2001; Rattay et al. 2001a). The majority of these values were obtained from guinea pig or gerbil animal models as human data are not available and were originally compiled from Strelioff (1973b), Spelman et al. (1982) and Finley et al. (1990). Some of these values, like that of perilymph, can be assumed to be fairly representative of the human case as the chemical composition of perilymph is fairly universal

[4] Multi-physics finite element analysis software. http://www.comsol.com/

across mammals. Other values, such as that of bone, may differ greatly from the human case as the density and porousness of bone varies between species. Micco et al. (2006) ascribed the difference in bone resistivity between the guinea pig and gerbil to this difference where the guinea pig has compact bone and the gerbil has thin and porous bone. This variation in values may be the reason why a large range of values have been used to describe cochlear bone in modelling studies.

Bone resistivity has been shown to significantly affect the predictions from 3D VC models (Kalkman et al. 2014b; Malherbe et al. 2015b) and the value thereof has been updated from the original value of 0.156 S/m to an order of magnitude lower based on electric field impedance measurements in implant users.

Kalkman et al. (2014a) optimised the conductivity of the modiolus to reflect fluid compartments in the structure, also based on electric field impedance measurements in users. Table 1 summarises the most common conductivity values that are currently used in VC models of the cochlea.

Table 1. Current conductivities of cochlear structures used in purely resistive 3D VC models of the cochlea. Recently updated values are indicated by an asterisk.

Cochlear structure	**Conductivity [S/m]**
Basilar membrane	0.0125
Bone	0.0154*
Brain	0.2
Metal electrodes	1000
Organ of Corti	0.012
Peripheral axons - axial	0.3333
Peripheral axons - transverse	0.067
Modiolus	0.3*
Reissner's membrane	0.000098
Scala Media	1.67

Scala Tympani	1.43
Scala Vestibuli	1.43
Scalp	0.33
Silicone rubber	1×10^{-7}
Spiral ganglion	0.3333
Spiral ligament	1.67
Stria vascularis	0.0053

Some researchers have argued that the capacitive effects of tissues, and especially the electrode-electrolyte interface, cannot be ignored in VC models of the cochlea. A study by Wong et al. (2015) investigated the effect of frequency dependence of tissue resistivities on the predicted potential waveforms. They modelled the stimulus as a biphasic constant current pulse that was represented by the sum of a number of Fourier harmonics. A 3D model of the cochlea was subsequently solved for a set of impedance values relevant to each harmonic and the resulting potential waveform was reconstituted by summing the results over frequencies. Considerable differences between the quasi-static and time-dependent formulations of the problem were found, especially in the nerve tissue that exhibited a substantial reduction in voltage magnitude over the duration of each phase of the waveform. This finding challenges the existing assumption that neural activation may be predicted by a quasi-static solution to the potential field predicted by a 3D FE model.

Choi et al. (2006; 2014) demonstrated the effect of the electrode-electrolyte interface on the prediction of electric field image data in 3D VC models of the cochlea. They implemented the interface though a simple lumped element model that consisted of a capacitor that represents the double layer capacitance of the electrode-electrolyte interface, and a parallel resistance that allows faradaic current injection. It is well-known that electrode impedance changes over time, whether caused by encapsulation of the electrode array

(Hanekom 2005; Newbold et al. 2014) or by a change in the properties of the electrode-electrolyte interface brought about by charge injection through the interface (Newbold et al. 2014).

These studies underscore the importance that the role of inclusion of time-dependent tissue characteristics, and especially a time-dependent description of the electrode-electrolyte interface play in prediction of neural excitation with 3D models and that this should be explored further. While purely resistive models have gained widespread acceptance because of their demonstrated ability to predict typical electric behaviour and neural responses to intracochlear electrical stimulation, they still lack robust predictive ability. This is especially important in the light of future development of models for specific live CI users that may be employed to optimise mapping parameters and diagnose problems with their implant.

Application of source and boundary conditions

The development of a 3D VC model is completed by application of boundary conditions. These include the specification of the source (the current or voltage applied to the active electrode) and sink (the grounding condition on the return electrode) as well as the conditions that apply at the boundaries between tissues and at the boundary of the model domain. It should be noted that cochlear implants usually stimulate with constant current and not voltage. Stimulation with current minimizes effects of the tissue impedance and a changing electrode-electrolyte impedance. A charge continuity condition is imposed on the boundaries among tissues while boundary conditions that are implemented on the model domain's outer boundary depend on the specific implementation of the domain surrounding the cochlear model.

The majority of 3D VC models of the electrically stimulated cochlea are either embedded into a finite (with air around, i.e. no charge continuity) or an infinite bone volume (i.e. charge continuity into an infinite domain) (Frijns et al. 2000b; Hanekom 2001; Malherbe

et al. 2015b). Recently the model domain was also implemented with an elliptic head model consisting of bone surrounded by air (Malherbe et al. 2015b), a basic head model consisting of skull, scalp and brain volumes (Malherbe et al. 2015b) and a detailed head model reconstructed from a sectional imaging process (Tran et al. 2014). Figure 3 shows the head model solved for stimulation with an electrode inside the cochlea.

Implementation of the return electrode, specifically for monopolar stimulation, proved to be an important factor in the prediction of both the potential field inside the cochlea as well as the resulting neural excitation profiles. The return electrode could be implemented to simulate an ideal spherical current return path by grounding the outer surface of a bone volume around the cochlear model, by applying the grounding condition to a part of the model, such as at the base of the cochlear nerve, or by implementing a realistic return electrode geometry into the VC description of the system. Recent studies have investigated the effect of the implementation of the return electrode on predictions from 3D VC models and found that it is necessary to include an accurate description of the return electrode geometry in these models to enable acceptable predictions of current paths through the cochlear volumes (Malherbe et al. 2015b; Tran et al. 2014; Wong et al. 2016).

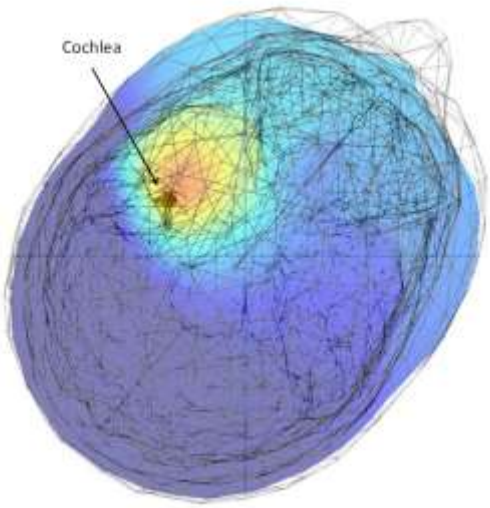

Figure 3. Head model with cochlea showing the potential field as a result of intracochlear stimulation.

Meshing and solving of the model and interpretation of results

While not necessarily reported, meshing of biological structures for numerical analysis is frequently a rigorous task that may require frequent intervention to sort out meshing errors. Built-in meshing algorithms in numerical modelling and analysis software packages have improved over the years, but complex geometries may sometimes require the use of dedicated meshing software to resolve the mesh. Many analysis software packages, such as Comsol and Ansys for finite element analysis, are available and the choice of modelling platform depends on the MGW that is followed to create the model. The output of a 3D VC model is a potential distribution throughout the modelled cochlea that may be used to assess the electric behaviour of the system, or that may be interpreted in terms of neural excitation behaviour through integration with a neural model. The approach to interpretation of results will become clear throughout the discussion of the various models that have been created and their application in the remainder of the article.

Landmark-based model generation workflow example

As an example of the workflow described above, this section presents the landmark-based MGW that is employed by the University of Pretoria group to construct user-specific models of living cochleae. Details about the specific implementation of this workflow may be found in Malherbe et al. (2013; 2015a; 2015b). The MGW inherently makes provision for an improvement of the integrity of the dimensional characteristics of the model with improved quality of the image data, but more importantly, it actively seeks to accommodate low-resolution data. It therefore does not limit the applicability of the technique to high-quality data, but allows a usable representation of the anatomic landmark features of the individual implanted system. This is important for a number of reasons. First, high-quality data sets are not always available, especially in developing countries. Second, older data sets obtained with lower-resolution technology may contain important information such as a clearer

delineation of the cochlear canals prior to ossification that may have taken place since acquisition of the image data. This argument also applies to pre-operative image data that are free from metal artefacts from the electrode contacts and may thus be registered with post-operative image data where aspects of the cochlear morphology may be obscured.

The image source data from which the models are constructed are clinically obtained CT data. An oblique reconstruction of a cube of approximately 50 mm side length around the inner ear is performed parallel to the basal turn of the cochlea (Connor et al. 2009). This image set is then resliced radially from the centre of the modiolus at 1 degree increments (angle θ measured from the centre of the round window) for 360 degrees. The result is a set of 360 mid-modiolar images from which the cochlear dimensions can be measured.

Landmarks that define the most distal boundary of the cochlear wall and the most superior boundary of the cochlear duct are measured and used as the base spirals around which the model is constructed. To extrapolate the apex boundaries (which are generally difficult to distinguish on CT images) and smooth out measurement errors introduced by the low resolution of the data, the measured landmarks are mapped onto template spirals that were obtained from cochleae illustrated in literature (Erixon et al. 2009). A procrustes approach is used to determine the best template to apply for this process.

The next challenge is to include inner-structure details that are not visible on conventional CT images either because the contrast is too low (as in the case of non-bony structures) or because the structures are comparable to or smaller than the voxel size of these images. Image registration between dimensions measured from a user's CT imaging data and a template model that was constructed from a mid-modiolar section through a human cochlea is used to augment the low-resolution CT data. The basic approach is to remap the template containing the inner structures so that its boundaries corresponded with the trajectory of the boundary template. This requires moving each cochlear duct until its outer boundary

intersects the template boundary. The final high-resolution representation of the cochlea containing the electrode array is constructed from the registered data set. An example of a user-specific model is shown in Figure 4.

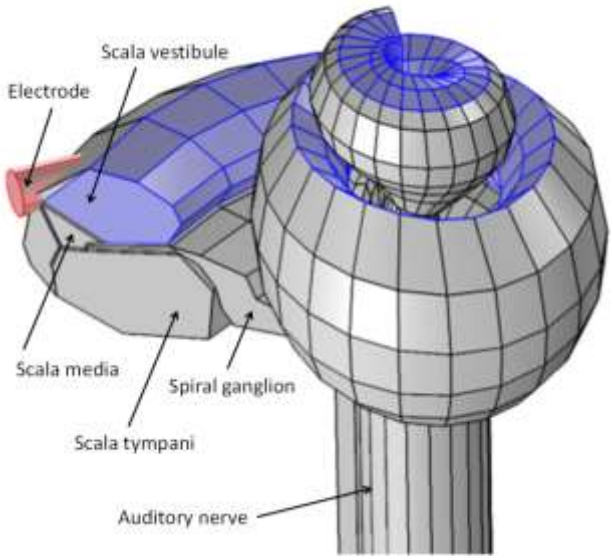

Figure 4. The model framework is used to define surfaces that delineate each structure, which are then exported to the finite element modelling software where volumes are created for volume conduction analysis. The figure shows a user-specific cochlear model with the electrode array (light red) where it enters the spiral. The scala vestibuli is shown in blue.

The user-specific models also include a description of the head volume, as it was shown that the specific implementation of the return electrode affects predictions about current distribution in cochlear models (Govindasamy 2012). The base model to describe the head volume is a generic head model that consists of the skull, brain volume and scalp. The dimensions of the structures are changed to reflect the size of the corresponding structures as measured from the CT data of the specific CI user.

Models in literature

Having considered the processing whereby 3D models are developed, the models that are available in literature are discussed next. While the ultimate goal of 3D models of the periphery is to investigate the relation between stimulus and response in human implantees, the fact that animal models have routinely been used to investigate the electrically stimulated mammalian auditory system experimentally, justified and drove the development of 3D models of animal cochleae. Because of the invasive nature of experimental animal models, 3D computational models of these animals have the benefit of using invasively measured data to inform the development of the computational description of the processes underlying peripheral auditory excitation. This approach provides a more dense representation of the peripheral auditory system than what is possible for living human models where data need to be collected through mainly non-invasive means. Ideally, some of the information density in these animal models may then be used to enrich the equivalent living human models. This also means that the development of animal models did not precede human cochlear models, but took place in parallel to either probe the electrophysiology of the auditory system or to inform the development of human models. In this section the different models that have been developed are reviewed, while the expression of the models in research and clinical application is explored in the next section.

Animal models

The most common animal model in CI research is the guinea pig because of the favourable trade-off among cost, quality of specimens and ease of performing micro-dissection and histologic procedures (Albuquerque et al. 2009). For this reason a number of guinea pig CI models have been published, e.g. the models by Frijns et al. (1995); Malherbe et al. (2013) and Wong et al. (2016)). Cat is also a popular experimental animal model (Hatsushika et al. 1990) for which a 3D model has recently been developed (Kang et al.

2015), while other experimental animal cochlear models like mouse (Irving et al. 2013), ferret (Hartley et al. 2010) and monkey (Pfingst et al. 1979) have not yet been described in 3D computational models.

The seminal work in animal modelling was done by Frijns and colleagues at the University of Leiden. In 1995, Frijns, de Snoo and Schoonhoven presented a rotationally symmetric 3D boundary element (BE) model of a guinea pig cochlea coupled with an active nerve fibre model (Frijns et al. 1995), which pioneered the integration of VC models with active neural models. The model was used to translate the potential distributions predicted by the VC models to neural response patterns and proved to be more accurate than the previous unrolled cochlear models. The geometry was constructed from a photomicrograph of a section through the second turn of a guinea pig cochlea by extruding the boundaries of the segmented image around the modiolus to create a rotationally symmetric structure. This approach was ideally suited to the BE method that allows for the discretisation of only a few surfaces instead of discretisation of a volume, as is the case with finite elements or finite differences. With this technique it is also possible to add a mesh afterwards, thereby avoiding rebuilding of the entire geometry when alterations are made (Briaire et al. 2000a). Model predictions proved to be in good agreement with published electrical ABR data.

This model was used to study the influence of temporal stimulus parameters and electrode configurations on the spatial selectivity of electrical stimulation (Frijns et al. 1996). This line of work was continued in 2000 with the extension of the model and the realisation of a 3D tapered spiral with macro electrodes and a procedure to generate the mesh to solve the electrical volume conduction problem (Briaire et al. 2000a), complemented by an article describing application of the model to predict the neural response to an arbitrary cochlear implant (Frijns et al. 2000a). The model first predicted the potential distribution through the cochlear volume and then applied a nerve fibre model to predict excitation profiles. An

evaluation of preferential current paths in a guinea pig cochlea model was investigated (Briaire et al. 2000b) and a comparison with the results with a human model, generated following the same procedure, was made (Frijns et al. 2001). Westen et al. (2011) used this model to test the hypothesis that ECAP amplitude is linearly related to the number of excited nerve fibres and found that this is only true at low stimulus intensities. The implication is that ECAP amplitude may not be a good predictor of objective mapping parameters such as maximum loudness level. This series of articles all described a generic representation of a guinea pig cochlea, as it extrapolated the findings based on a single geometry to typify the biophysical behaviour of the auditory periphery.

In 2013, the development of a subject-specific model based on µCT data was reported by the University of Pretoria group (Malherbe et al. 2013) as a first step towards the establishment of a MGW for user-specific models for live users. The objective was to investigate the factors that would allow prediction of user-variability in outcomes. The model was developed from a µCT image stack of a guinea pig cochlea[5]. Electrophysiological responses measured from the inferior colliculus of the same animal were available for validation of model outcomes. A method was proposed whereby anatomical details such as the geometric properties of the organ of Corti and the basilar membrane could be registered with a representation of the cochlea obtained from a landmark digitisation procedure to increase the feature density of the model. The work was extended by a study by Govindasamy (2012) that emphasised the importance of including a fair amount of detail into user-specific models, such as an accurate description of the return electrode and the electrode carrier.

5 Image stack obtained from collaborators at Epstein Laboratories at the University of California San Fransisco.

A highly detailed model of a guinea-pig cochlea, including details of the major blood vessels in the cochlea, was recently presented by Wong et al. (2016). The MGW to create the level of detail demonstrated in the model was first described by Tran et al. (2014) and is based on an intricate fusion of manual and semi-automatic segmentation and volume rendering steps. The study sought to validate the 3D VC modelling approach against independently obtained in vivo voltage tomography data. Results suggested that intra-scalar voltages predicted by the model were more sensitive to the choice of boundary condition than to the assigned tissue resistivity values although potential distributions at the neurons were affected by the resistivities of bone, perilymph, and nerve. The study demonstrated a strong correlation with the in vivo voltage data, supporting the validity of the 3D VC approach to cochlear modelling.

The most recent addition to the animal model repository in terms of species is a 3D model of a cat cochlea developed by Kang et al. (2015). This model was used to evaluate the effects of electrode position on the auditory nerve fibre response. The model extruded a simple geometric representation of a section through a cat cochlea in a spiralling fashion, similar to the approach by Briaire et al. (2000b) and Hanekom (2001). The primary objective of the model was not to create a high-fidelity anatomical representation of the cochlea, but rather to generalise the finding that electrode position affects the spatiotemporal pattern of the neural response and to show that this effect is dependent on stimulus rate. Model predictions could be validated against invasively measured neural response data reported in literature.

Human models

The first 3D human VC model preceded animal models by almost a decade with the study by Girzon (1987) . The model that was based on the method of finite differences could show that the distribution of the electric potential along the scala tympani was asymmetric and it could predict the potentials resulting from intracochlear stimulation in the vicinity of

the neurons. However, it did not provide sufficient resolution to allow integration with neural models and was soon followed by the model of Finley et al. (1990) that included the first rudimentary description of neural responsiveness to the predicted potential distributions. The activating function (Rattay 1986) was used to predict the origin of spike generation amongst four modelled locations for nodes of Ranvier. A preliminary investigation on the possible integration of active membrane models with the VC model was also presented and prompted the development of the integrated VC-ANF model of the guinea pig cochlea by Frijns et al. (1996) six years later.

In 2001, three generalised human cochlear models were published. The BE model by Frijns et al. (2001) presented a spiralling 3D representation of the human cochlea constructed from histologic data. This model was used to investigate spatial selectivity and dynamic range that typifies cross-turn stimulation with the intention of improving understanding of the stimulation characteristics of modiolus-hugging electrodes. It was shown that the model was appropriate for testing and comparing of different electrode designs under identical and controlled circumstances. A subsequent study extended the model to facilitate an inverse calculation of the contribution of single fibre action potentials (SFAPs) to the measured ECAP. The model predicted that the measured ECAP may not necessarily reflect the action potential that propagates along the auditory nerve.

The human model presented by Hanekom (2001) employed the FE method and represented the basal one-and-a-half turns of the cochlea. The model was created by extruding a section through a turn of a human cochlea around the modiolar axis and thus did not include geometric asymmetries. The model predicted potential distributions as a result of intracochlear stimulation and the resulting neural excitation. It included the spiralling nature of the cochlea and facilitated modelling of different electrode geometries, array locations and electrode separations without the need to regenerate the mesh. Three different shapes of

electrode contacts could be configured (full-band, half-band and a square contact that approximated a ball electrode) which could either be recessed or level with the carrier. It was concluded that the 3D location of the electrode contacts inside the scala tympani has a marked influence on the excitation site and is a primary parameter in the control of excitation spread. The study confirmed observations that threshold currents may be reduced by placing the electrode array closer to the modiolus and that the spiralling geometry of the cochlea results in asymmetric potential distributions. The model was subsequently applied to investigate the effect of encapsulation tissue around the electrode array (Hanekom 2005).

The spiralled model by Rattay et al. (2001a) was based on a photograph of a midmodiolar histological section through a human cochlea. The primary objective of the model was to generate appropriate voltage distributions to validate a new compartmental neural model presented in a companion article (Rattay et al. 2001b) and to assess its effectiveness in predicting excitation characteristics of intracochlear stimulation. The model confirmed observations that voltage decay is more rapid in the basal turn due to the larger size of the scala tympani in this region, and showed that apical nerve fibres may typically be excited within the modiolus and not at the periphery. The model also showed that the site of excitation along the nerve fibre is reflected in a delay of the neural response, i.e. responses generated peripherally are delayed relative to responses elicited in the modiolus. This may confound temporal characteristics that could be transferred by a cochlear implant for users that have surviving dendrites in the organ of Corti. The study also investigated the focusing properties of different electrode configurations on neural excitation and found that intra-scalar return electrodes should allow more focusing than monopolar stimulation.

Choi et al. (2005; 2014) created a model that is based on the geometry of a section through the human cochlea presented in the model of Hanekom (2001). The model was constructed by extruding the geometry along various circular and spiralling trajectories. They

used the models to compare neural excitation characteristics of different cochlear implant electrodes and found that planar electrodes create more focused potential fields than banded or halfband electrode contacts, consistent with other reports in literature. The effect of inclusion of the electrode-tissue interface into 3D VC models was also investigated (Choi et al. 2006) and this showed that the frequency characteristics of the interface is important for the accurate prediction of the electric field image data measured by Vanpoucke et al. (2004b). In a subsequent study, the conditions for creating virtual channels amid neighbouring electrodes through controlled channel interaction was investigated, and the authors could show that a broad excitation pattern is necessary to produce the kind of electrode interaction necessary to form distinct virtual channels (Choi et al. 2009). The most recent application of this model was to investigate the origins of the ECAP. Good correspondence between measured and predicted ECAPs could be demonstrated by modelling the path between the neural nodes and the measuring electrode by an equivalent RC electric circuit that captures the properties of the electrode-tissue interface.

The model by Ceresa et al. (2015) was based on a single high-resolution µCT scan of a cadaver cochlea and was aimed at optimising neural excitation based on an ideal excitation metric by manipulating stimulation parameters. The representation of the cochlea was limited to a duct divided by a bony septum at the location of the spiral lamina. Whether the proposed metric will yield improved perceptual results on a user-specific basis remains to be seen, as the analysis was limited to a single test case.

Dang et al. (2015) also based their model on geometric parameters obtained from µCT images of a cadaver cochlea. They presented a parametric 3D model that used the µCT images to adapt the geometry. Model predictions proved to be in good agreement with multi-channel stimulation data measured from the implanted cochlea. The results confirmed that electric field distribution is affected by the shape of the cochlea.

The 3D models of the human auditory periphery described up to this point focused on generalisation of predictions based on a single cochlear morphology and are in essence generic 3D models. These models attempted to explain typical behaviour that is observed over a general population of CI users. The first study to investigate the effect of individual morphology on predictions made by 3D models was conducted by Whiten (2007). The approach was to develop detailed models of the cochleae of two deceased implant users from images of histologic sections of their temporal bones. Model predictions were compared to data from the literature, a cohort of implanted research subjects and archives collected during the years of CI use of the modelled CI users. The comparisons to archival data showed promising correspondence between model-predicted and empirically-measured data. This suggested that representation of user-specific characteristics in 3D models may affect prediction and may offer improved prediction of user-specific outcomes when compared to generic models.

Morphologic variation was also included by Kalkman et al. (2014a) who modelled four different cochlear geometries to probe place pitch. Because the models were based on histologic sections through human cochleae, it was possible to extend human models to include detail about the fluid compartments in the modiolus. Electrical conductivity values of bone and the modiolus were also updated based on clinical data. To make an accurate assessment of place pitch, the bicycle spoke trajectories of the dendrites reported by Stakhovskaya et al. (2007) as well as the displacement of their cell bodies towards lower turns were implemented for apical neurons. Model predictions confirmed the validity of pitch estimation in the basal turn of the cochlea by application of Greenwood's function (Greenwood 1990), but showed that pitch becomes increasingly unpredictable towards the apex, relying on the specific combination of stimulus level, state of the cochlear neurons and the electrode's distance from the modiolus at the point of interest. The model was further

applied to investigate multipolar current focussing strategies and results confirmed the role of electrical field interaction to induce spatially restricted excitation patterns. The implication is that perimodiolar electrodes may be too close to the target neurons to allow field interaction and therefore a summed spatial excitation profile. This is consistent with the analysis of Choi et al. (2009). The model also showed the 3D spatial penetration patterns of neural excitation into the spiral ganglion, which is among others important for interpretation of pitch percepts with cochlear implants.

The first attempt at modelling of live users' cochleae was presented by Malherbe et al. (2015a; 2015b). The construction of these models were discussed in the previous section as an example of the application of the MGW by which 3D VC models of the human periphery may be created. The primary challenge that needs to be contended with in the development of 3D models of live cochleae is inadequate resolution of image data from which user-specific morphologic characteristics need to be extracted. These two studies showed that spread of neural excitation is highly dependent on cochlear morphology. Model predictions of the effect of cochlear morphology were compared to the predicted effect of medial versus lateral placement of electrodes in the scala tympani. While the latter is known to be one of the primary factors that affect excitation thresholds, estimates from the models suggest that the effect of cochlear morphology on excitation thresholds is two-thirds as large as that of medial-lateral electrode placement. This has important implications for models that aim to predict user-specific outcomes.

Neural models

As noted previously, a complete description of the biophysical interface requires an interpretation of potential distributions in terms of neural excitation characteristics. The majority of models discussed above have been coupled to some form of interpretive neural description. Prediction of neural excitation can be coupled to VC models on different levels.

At its most basic level, neural excitation may be probed using the activating function (Rattay 1986) which is the second spatial derivative of the potential field on a plane that intersects the nodes of Ranvier. Examples of where this approach was employed are the models of Finley et al. (1990), Rattay et al. (2001a) and Nicoletti et al. (2013). The activating function assumes that the neuron is in the resting state and only indicates the direction and degree to which the node is inclined to change from the resting state. It can neither predict the firing threshold nor any temporal behaviour (e.g. temporal integration or adaptation). To this end the activating function is useful for qualitatively probing the spatial location and extent of neural excitation.

Neural models that have most commonly been combined with VC models are physiologically-based active membrane neural models that depend on the extracellular potential gradient that is predicted by VC models. Such a model may straightforwardly be integrated with a VC model as long as the VC model can predict the potentials at the specific locations of the nodes of Ranvier. This family of models include the compartmental of Rattay employing the Hodgkin-Huxley membrane equations (Rattay et al. 2001b) and the generalised Schwartz-Eikhof-Frijns model (Frijns et al. 1996) which uses an adaptation of the original Schwartz-Eikhof membrane model. The latter has been revised twice to more strongly incorporate human characteristics (Briaire et al. 2005; Kalkman et al. 2014a). This class of models can potentially provide a very rich description of the neural behaviour depending on its predictive capabilities. Predictions include temporal behaviour such as adaptation and derived measures such as the prediction of ECAPs (Briaire et al. 2005; Rubinstein 2004) and the factors from which latencies in neural responses originate (Rattay et al. 2001b).

The main disadvantage of physiologically-based active membrane neural models is their computational intensiveness which implies excessive simulation times especially when populations of neurons are modelled. The computational cost further increases with the

addition of stochastic properties to physiologically-based models. Integration of analytical models of neural behaviour into VC models of the cochlea may thus provide an alternative, computationally less-expensive description of neural behaviour to electrical stimuli. The single fibre stochastic model of single biphasic-pulse excitation of auditory neurons by Bruce et al. (1999b) and the subsequent pulse-train formulation of the model (Bruce et al. 2000) provide an accurate and computationally efficient description of neural excitation properties. The stochastic models have been successfully applied to predict behavioural threshold, dynamic range and intensity difference limen (Bruce et al. 1999a) for single pulses and behavioural threshold for pulse trains (Xu et al. 2004).

Validation of models and model parameters: probing biophysics in the research domain

An important aspect of 3D modelling is validation of the models in terms of measurable quantities. Since 3D models provide a description of the periphery of the auditory system, their output must either be assessed at the level of output, i.e. in terms of the electric potential field that it generates in response to electrical stimulation, or their output needs to be interpreted in terms of higher level responses. Combining a neural model with the VC models allows interpretation of the potential fields in terms of neural excitation profiles. However, because of the small dimensions of the cochlea, the delicacy of its structures and its surgically inaccessible location, it is difficult to take direct measures of neural excitation on a single fibre level. Derived measures are thus frequently employed that reflect the activity at the periphery. The drawback of derived measures is that they add another level of complexity to the models since the derivation needs to be included in the structure of the model. An example of this is the electrically evoked compound action potential (ECAP) that is the potential that can be measured at an electrode as a result of the combined activity of all the

nerve fibres that were activated by a stimulus. To be able to validate a model against such a measure, the mechanisms for detection of the ECAP needs to be included in the model as demonstrated by Westen et al. (2011). While this may extend the applicability and predictive scope of a model and thus the set of measures against which it may be validated, additional layers of complexity often introduce more uncertainty in the predicted quantities. This is also one of the main reasons why care must be taken when extrapolating predictions from 3D models to perceptual outcomes. Without a thorough description of the central processes that translate the output from the periphery to percepts it is inadvisable to validate 3D model outputs against perceptual measures.

Since animals may be subjected to invasive measurements to characterise the functioning of the neurophysiology, the level of validation that is possible with animal models is deeper than what is possible for human models where invasive measurements may only be performed on cadavers that lack neural responsiveness. Typical measures that are available for validation of 3D electro-anatomical models are summarised in Table 2 with references to examples of studies that either describe them or have employed them for validation.

Table 2. Typical measures for validation of 3D models.

Measure	Live human	Animal or cadaver	Description
In situ electric potential measurements	×	✓	Physical measurement of potentials inside the cochlea. These may be directly compared to predicted potential values. (Black et al. 1983; Dang et al. 2015; O'Leary et al. 1985)
Single fibre or cluster responses from the inferior colliculus (IC)	×	✓	Neural responses in the form of IC recordings may be measured from live animal subjects. Since tonotopicity is maintained, the measured responses provide an indication of

			the peripheral neural response, which may in turn be predicted by a neural model combined with 3D VC models. (Malherbe et al. 2013)
ECAP	✓	✓	The electrically evoked compound action potential (ECAP) is the sum of the neural activity detected at the electrodes in response to an electrical stimulus. It is a standard clinical measure. (Choi et al. 2014; Westen et al. 2011; Whiten 2007)
EFI	✓	✓	Electric field imaging measures the voltage distribution as a function of the electrode position in the cochlea in response to the stimulation of a single electrode. This may be directly compared to predictions of potentials at the electrode contacts in a 3D VC model. (Choi et al. 2006; Lau et al. 2011; Malherbe et al. 2015b; Vanpoucke et al. 2004a)
Map parameters: Perceptual thresholds (T), Comfort level (C) and dynamic range	✓	✓	T levels are the lowest current levels at which a percept is elicited while C levels are the current levels at which the maximum comfortable loudness of a percept is elicited. Dynamic range is the difference between these two measures. Snel-Bongers et al. (2013) proposed a 1 mm region of excitation as an indication of perceptual threshold levels and a 4 mm region of excitation as an indication of perceptual C levels. The predicted current that excites a 1 mm region (T) or 4 mm region (C) of nerve fibres is excited may be compared to T and C levels recorded in the maps of users. These measures may be unreliable since they are a perceptual interpretation of the model output. (Malherbe et al. 2013; 2015a)

Application of models: predicting current spread

A primary objective of 3D models is to predict and understand voltage and current distributions in the cochlea, and the resulting neural excitation patterns. Interaction between electrode stimuli may be in the form of electrical interactions between electrodes (Boëx et al. 2003), and may also result in neighbouring electrodes stimulating overlapping neural populations (neural interaction). Current spread is important, because this limits spatial resolution of stimuli in cochlear implants, and this may in turn result in spectral smearing of the electrically-elicited spectral representation and may limit the number of independent information channels (Strydom et al. 2011). This effect is especially important in simultaneous stimulation, but interaction also occurs for non-simultaneous stimulation (Boëx et al. 2003). Current spread, current decay rate away from the stimulation electrode, voltage distribution and extent of the region of neural excitation (or spread of excitation) are all related, but different ways of expressing the effect of the electrical stimulus that may be observed some distance away from the electrode.

Current decay has been measured in saline bath experiments, with estimates of current decay of 2-4 dB/mm for bipolar stimulation and 0.5 to 1 dB/mm for monopolar stimulation (Black et al. 1983), and O'Leary et al. (1985) finding current decays of 2-3 dB/mm for Nucleus CI22 bipolar electrodes. However, Kral et al. (1998) showed that while tank measurements corresponded to cadaver measurements in the basal part of the cochlea, but more apical decay values are larger in cadavers. Spatial resolution becomes better towards the apex. Moreover, in vivo cat neural excitation data (Hartmann et al. 1990; Kral et al. 1998) show decay rates of 3 dB/mm for monopolar sinusoidal stimulation, and 7.4 to 8.5 dB/mm for bipolar stimulation, underlining the importance of coupling of volume conduction models and neural models in 3D models. Measurements typically show asymmetry in the spread of

excitation, especially in monopolar configurations, and also wider potential distributions around basal electrodes (Kral et al. 1998).

Predictions from 3D models approximate the measurements mentioned above. Models show that potential distributions vary among the different modes of stimulation (different bipolar stimulation modes in which active and return separations vary, and monopolar stimulation; Kral et al. 1998). The spiralling finite-element model of Hanekom (2001) showed average values of current decay of 7.5–10 dB/mm for bipolar stimulation, and around 2 dB/mm for monopolar stimulation. Model-predicted spread of excitation differs in apical and basal regions of the cochlea, shown in the 3D model of Hanekom (2001), but also in the lumped parameter model of Kral et al. (1998).

While predicted trends in models correspond to the available measurements in broad terms, models have extended our understanding of the origins of current spread. Models clearly show that the geometry of the cochlea is important, with generic models showing, for example, that the spread of current is higher in the basal turns of the cochlea. This may be because of the wider cochlear duct (Kral et al. 1998) or the spiral shape of the cochlea, with the radius larger in the basal region than in the apical region (Hanekom 2001). In addition, the model of Hanekom (2001) showed that spread of excitation of laterally positioned electrode arrays increases significantly at wide bipolar electrode separations, and that the most effective way to control spread of excitation is to locate electrodes close to the target nerve fibres.

Although current decay is often approximated as a simple exponential decay, Briaire et al. (2000b) have shown in their rotationally symmetric 3D model that this approximation only holds in the far field. Current decay is higher close to electrodes, seen also in the model predictions of Hanekom (2001). Briaire et al. (2000b) have shown that current decay follows an inverse square law along the scala tympani in the immediate vicinity of the electrode.

Additionally, the extent of current spread is determined by the electrode configuration, characteristics of the medium, the distance from the stimulating electrode and the geometry of the medium and the electrodes (Frijns et al. 1995; Hanekom 2001). The spreading characteristics of the medium depend on a number of parameters, including material properties of the perilymph, endolymph, spiral ganglion and basilar membrane. These are typically included in 3D models (Frijns et al. 1995; Hanekom 2001; 2005).

Cohen (2009) showed that the spread of the effective stimulation field (ESF), which is defined as the ability of the field to excite neurons, is a function of the longitudinal distance between an electrode and the target neurons, i.e. the user-specific effects of electrode array type and position on the ESF. He used spread of excitation derived from ECAP masking functions and predictions of the spread of the electric field inside the cochlea from a simple axi-symmetric finite element model of the cochlea to derive the ESF. This demonstrated that current decay (interpreted as the ESF in Cohen's model) is a function of the position of a specific electrode within the cochlea. Applying the model of Malherbe et al. (2015a), and systematically applying point source stimuli at different positions along the length of the scala tympani, and at difference distances to the scala walls at each scala tympani position, we calculated the voltage decay rate from current sources at each of these positions. This was done for each of the five implanted cochleae modelled by Malherbe et al. (2015a). The resulting potential distribution of each source position was considered at the first nodes of each neuron at the modelled neuron locations, described in Malherbe et al. (2015a). These nodes were positioned in the neuron region in the spiral lamina just medial to the organ of Corti.

These simulations showed that voltage decay was a function of several cochlear morphological parameters as well as electrode placement within the scala tympani. While decay in a longitudinal direction (along the scala tympani) and a radial direction were both

predicted to be exponential, these decay rates differed. Also, voltage decay rate was sensitive to cochlear size (parameterised by cochlear base width), duct cross-sectional area, duct height, duct width, position of the current source along the length of the scala tympani, distance of the source to the modiolus, distance to the medial and lateral walls and distance to the organ of Corti. For example, it was found that longitudinal current decay rates varied with radial position (distance to modiolus) of the source. This electrode position and cochlear geometry sensitivity underlines the importance of models that are user-specific.

Application of models: the clinical domain

A useful measure of how effective cochlear implants are in restoring hearing in an individual CI user is often difficult to attain as the level of benefit may be difficult to characterise in spite of satisfactory clinical outcomes. The description of a user's cochleae through 3D computational models is therefore clinically relevant as it may enable clinicians to gain insight into the workings of the electrically stimulated cochlea. Translation of 3D CI models to the clinical domain is further promoted by the drive towards user-specific models that incorporate the specific morphology of an individual's cochlea and location of the electrode array.

The development of 3D cochlear models has provided much insight into the behaviour of the auditory periphery in reaction to electrical stimulation, including an understanding of the relationship between the distance of the electrode from the surviving nerve fibres and thresholds, the focusing ability of various electrode placements and electrode designs, ectopic excitation and the factors that affect this, the origin and characteristics of the ECAP, and frequency mapping in cochlear implants. In addition, the predictive ability of these models has improved to the point where they may soon become clinically applicable on a broad scale (Malherbe et al. 2015a). This is especially true with the escalation in the power of computational resources that allow cochlear models to be created with increasing levels of

detail and intricacy, and to be solved with growing accuracy while reducing computational time.

As mentioned before, deriving conclusions about perception based on predictions from peripheral models must be approached with care. However, since peripheral neural behaviour underlies perception, knowledge that may be gained through a 3D interpretation of the periphery may provide insight into the manipulations that may be required or experimented with to optimise the input to the central auditory system. An example is modelling of channel interaction that provides insight into possible effects thereof on perception.

A model-based clinical toolset that flows naturally from the objectives and predictive ability of 3D models of the electrically stimulated cochlea includes model-based visualisation (MBV), model-predicted mapping (MPM) and model-based diagnostics (MBD). Each of these are briefly explored in the following paragraphs.

Model-based Visualisation (MBV)

Visualisation of the cochlear implant electrode is routinely done via post-operative X-ray imaging, and in some cases via post-operative computed tomography (CT) imaging of the user's cochlea. Neither of these techniques provides a clear view of the electrode array's position. For the X-ray images, the three-dimensional nature of the array trajectory is lost while CT-images provide low-resolution visualisation that is further degraded by the presence of metal artefacts from the electrode contacts. Much research has been done on determining the trajectory of the electrode array inside the cochlea of an implant user (Gstoettner et al. 1999; Ketten 1994; Marx et al. 2014; Noble et al. 2010; Shpizner et al. 1995; Skinner et al. 1994; Verbist et al. 2008; Whiting et al. 2008), but this information generally does not contain a description of the inner structures of the cochlea. Visualisation

of the electrode array relative to cochlear structures may thus prove to be an informative by-product of user-specific 3D models. Figure 5 below illustrates the value of the approach.

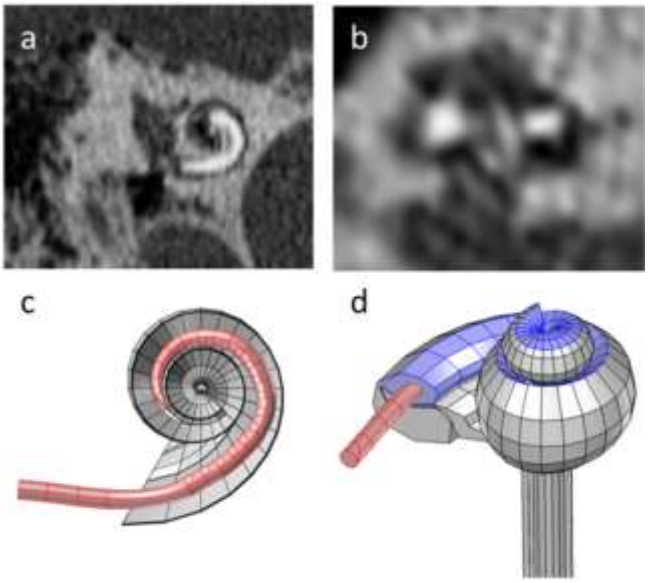

Figure 5. (a) Oblique view of the cochlea on a clinically obtained spiral CT image. (b) Mid-modiolar section through the same cochlea. (c) Visual rendering of the electrode inside the cochlea with structures removed to enhance visibility. (d) The complete model showing the electrode to be located in the scala vestibuli as a result of insertion through an incorrect cochleostomy site.

Model-predicted Mapping (MPM)

The use of 3D models may inform the optimisation of mapping parameters based on knowledge of, for example, the field interactions among different electrode configurations and stimulus paradigms, the neural population that is targeted by a specific electrode configuration and how it changes with increasing or decreasing stimulus level, and the relation between thresholds of different electrodes. An example is found in the recent study of Malherbe et al. (2015a) that showed how the centroid of the spread of excitation changes with increasing stimulus level and that is therefore expected to cause changes in perceived pitch. While pitch shift with intensity increase is a known phenomenon (Arnoldner et al. 2008), a user-specific model may provide a rough quantitative indication of the magnitude of

the shift that may be produced under specific stimulation conditions for a specific electrode configuration. Another example is demonstrated in the same article where the excitation profiles for electrodes at the same angle of insertion in the two cochleae of a bilateral implant user were compared. For the CI users in that study, predicted excitation patterns for one of the two users at a specific angle were similar (this user's electrode arrays were in similar intracochlear locations) while the other had a medial electrode location in the one ear and a lateral location in the other resulting in strikingly different neural excitation patterns. Information like this may be valuable to inform and optimise the user's map, for example by attempting to compensate for frequency offsets introduced by dissimilar electrode insertions in the left and right ears of bilateral implant users, or to enhance the binaural cues that may be available in neural spike trains elicited by bilateral implants. Along these lines, Nicoletti et al. (2013) developed a model to investigate to which extent bilaterally implanted ears may be able to convey binaural information. The peripheral part of their model, more primitive than recent 3D cochlear models, did not consider the coiling of the cochlea, and assumed a current decay of 1 dB/mm. The modelled current was used as input to a Hodgkin-Huxley type neural model that modelled a population of 6000 spiral ganglion cells with varying properties. Predicted neural spiking patterns of two simulated ears were used as input to coincidence detection neurons that essentially calculated a cross-correlation between spike trains arriving from the two ears. This could then be used to investigate the ability of different speech processors to potentially convey binaural cues. Although not considered by Nicoletti et al, this approach may potentially be used to assist in map corrections to enhance binaural cues.

Ultimately, models need to predict speech perception abilities of individual CI users implanted with specific devices, given a number of user-specific parameters (including electrode type and positioning, speech processor and map parameters). This requires more advanced neural models that include modelling of central processing. An example of the

latter appears in Fredelake et al. (2012), who developed a model to predict speech perception. Their simple peripheral cochlear model implemented an exponential current decay, and the effective current at modelled leaky integrate-and-fire neurons caused these to produce neural spike trains. Spike trains were processed in a model of central auditory processing that included spatial, temporal integration and internal noise to form an internal representation. Stored internal representations were then compared to internal representations of words presented in noise, and speech reception thresholds (SRTs) were calculated. It would be possible to predict user-specific SRTs, knowing a number of user-specific parameters. Being able to predict speech perception outcomes for individual CI users will allow optimisation of maps for individual users.

Model-based diagnostics (MBD)

To date a number of 3D CI models have been developed for research purposes. However, very few have been applied to CI diagnostics. To be able to use 3D models in a diagnostic application, it is necessary to have a user-specific model, which perhaps explains the absence of diagnostic applications in the literature to date. An example of a diagnostic application of 3D models is probing the factors that may lead to changes in thresholds over time which could cause hearing performance to deteriorate. The source of changes may first be investigated, e.g. by assessing the effect of fibrous tissue encapsulation of the electrode, ossification of the cochlea or neural degeneration, in an attempt to diagnose the origins of the problem. This may be followed by an investigation of measures that may improve hearing performance such as remapping of the device based on the model-based diagnosis. The potential impact of this approach on the management and maintenance of hearing performance in CI users provides a strong motivation to pursue the development of the diagnostic application of 3D models.

The future of 3D models

While there has been consistent activity in the field of 3D models of cochlear implants over the past two decades, the realisation that the refinement of these models to include user-specific traits may shed light on the factors that underlie inter-person variance has stimulated new interest in the application and refinement of these models. It is suggested that the past role that generic models played in the description of general trends in the neurophysiological behaviour of CI-elicited hearing may conceivably be supplanted in future by statistical analyses of the predicted responses of a collection of user-specific models. To this end the development of a significant number of hi-fidelity user-specific models from cadaveric materials will play an important role in the future application of 3D CI models.

The development of a model-based clinical toolset is also a strong motivator for the refinement of models of specific live users. These models will become more accurate in future as imaging technology develops to allow more of the intricate details of the cochlear structure to be visualised in vivo. To support clinical availability, it is important to optimise the MGW to be able to produce user-specific models of living cochleae within a reasonable time with a reasonable amount of effort.

Looking back on the comment by Finley et al. (1990) that the stimulated cochlea "appears to be a highly non-linear, uncontrollable interface that limits the ultimate performance goals of cochlear prostheses" when considered as a whole, but that it can be separated into an ordered set of biophysical mechanisms, it is clear that 3D models are well-suited to probe and detangle the intricacies of this interface.

Acknowledgements

The authors wish to acknowledge the postgraduate students in Bioengineering at the University of Pretoria for their assistance in amassing some of the literature from which this review was written. They are: Tiaan Malherbe, Larry Schmidt, Alex Oloo, Johannes Myburgh, Liza Blignaut, Liezl Gross, Johanie Roux, Riaze Asvat, Rene Baron, Werner Badenhorst, Heinrich Crous and Flavio de Luca.

References

Adunka O, Kiefer J. 2006. Impact of electrode insertion depth on intracochlear trauma. Otolaryngology - Head and Neck Surgery 135(3):374-382.

Albuquerque AAS, Rossato M, De Oliveira JAA, Hyppolito MA. 2009. Understanding the anatomy of ears from guinea pigs and rats and its use in basic otologic research. Brazilian Journal of Otorhinolaryngology 75(1):43-49.

Arnoldner C, Riss D, Kaider A, Mair A, Wagenblast J, Baumgartner W-D, Gstöttner W, Hamzavi J-S. 2008. The intensity-pitch relation revisited: Monopolar versus bipolar cochlear stimulation. The Laryngoscope 118 (9):1630-1636

Black RC, Clark GM, Tong YC, Patrick JF. 1983. Current distributions in cochlear stimulation. Annals New York Academy of Sciences:137-145.

Blamey P, Arndt P, Bergeron F, Bredberg G, Brimacombe J, Facer G, Larky J, LindstrA m B, Nedzelski J, Peterson A et al. . 1996. Factors Affecting Auditory Performance of Postlinguistically Deaf Adults Using Cochlear Implants. Audiology and Neuro-Otology 1(5):293-306.

Boëx C, de Balthasar C, Maria-Izabel K, Pelizzone M. 2003. Electrical field interactions in different cochlear implant systems. Journal of the Acoustical Society of America 114(4):2049-2057.

Bookstein FL. 1997. Shape and the Information in Medical Images: A Decade of the Morphometric Synthesis. Computer Vision and Image Understanding 66(2):97-118.

Briaire JJ, Frijns JHM. 2000a. 3D mesh generation to solve the electrical volume conduction problem in the implanted inner ear. Simulation Practice and Theory 8(1-2):57-73.

Briaire JJ, Frijns JHM. 2000b. Field patterns in a 3D tapered spiral model of the electrically stimulated cochlea. Hearing Research 148(1-2):18-30.

Briaire JJ, Frijns JHM. 2005. Unraveling the electrically evoked compound action potential. Hearing Research 205(1-2):143-156.

Briaire JJ, Frijns JHM. 2006. The consequences of neural degeneration regarding optimal cochlear implant position in scala tympani: A model approach. Hearing Research 214(1-2):17-27.

Bruce IC, Irlicht LS, White MW, O'Leary SJ, Clark GM. 2000. Renewal-process approximation of a stochastic threshold model for electrical neural stimulation. Journal of Computational Neuroscience 9(2):119-132.

Bruce IC, White MW, Irlicht LS, O'Leary SJ, Clark GM. 1999a. The effects of stochastic neural activity in a model predicting intensity perception with cochlear implants: low-rate stimulation. Biomedical Engineering, IEEE Transactions on 46(12):1393-1404.

Bruce IC, White MW, Irlicht LS, O'Leary SJ, Dynes S, Javel E, Clark GM. 1999b. A stochastic model of the electrically stimulated auditory nerve: single-pulse response. Biomedical Engineering, IEEE Transactions on 46(6):617-629.

Cannon MWJ. 1976. Electrical impedances, current pathways, and voltage sources in the guinea pig cochlea. Syracuse, New York: Institute for Sensory Research, Syracuse University.

Ceresa M, Mangado N, Andrews RJ, Gonzalez Ballester MA. 2015. Computational Models for Predicting Outcomes of Neuroprosthesis Implantation: the Case of Cochlear Implants. Molecular Neurobiology 52(2):934-941.
Chaturvedi A, Mohan C, Mahajan S, Kakkar V. 2006. Imaging of cochlear implants.
Choi CTM, Hsu CH. 2009. Conditions for generating virtual channels in cochlear prosthesis systems. Ann Biomed Eng 37(3):614-624.
Choi CTM, Lai WD, Chen YB. 2005. Comparison of the electrical stimulation performance of four cochlear implant electrodes. IEEE Transactions on Magnetics 41(5):1920-1923.
Choi CTM, Lai WD, Lee SS. 2006. A novel approach to compute the impedance matrix of a cochlear implant system incorporating an electrode-tissue interface based on finite element method. IEEE Transactions on Magnetics 42(4):1375-1378.
Choi CTM, Wang SP. 2014. Modeling ECAP in cochlear implants using the FEM and equivalent circuits. IEEE Transactions on Magnetics 50(2).
Cohen LT. 2009. Practical model description of peripheral neural excitation in cochlear implant recipients: 2. Spread of the effective stimulation field (ESF), from ECAP and FEA. Hearing Research 247(2):100-111.
Community TA-CI. Cochlear Implant Statistics [Internet]. Available from: http://aslci.blogspot.co.za/2008/03/cochlear-implant-statistics.html
Connor SE, Bell DJ, O'Gorman R, Fitzgerald-O'Connor A. 2009. CT and MR imaging cochlear distance measurements may predict cochlear implant length required for a 360 degrees insertion. AJNR Am J Neuroradiol 30(7):1425-30.
Dang K, Clerc M, Vandersteen C, Guevara N, Gnansia D. In situ validation of a parametric model of electrical field distribution in an implanted cochlea. International IEEE/EMBS Conference on Neural Engineering, NER; 2015. p. 667-670.
De Quesada S. Statistics and notes about cochlear implants as of 1995 [Internet]. Available from: http://www.zak.co.il/d/deaf-info/old/ci-facts
Disorders NIoDaOC. 2011. NIDCD fact sheet: Cochlear implants. In: Disorders NIoDaOC, editor.
Disorders NIoDaOC. Cochlear Implants [Internet]. Available from: http://www.nidcd.nih.gov/health/hearing/pages/coch.aspx
Drennan WR, Oleson JJ, Gfeller K, Crosson J, Driscoll VD, Won JH, Anderson ES, Rubinstein JT. 2015. Clinical evaluation of music perception, appraisal and experience in cochlear implant users. International Journal of Audiology 54(2):114-123.
Erixon E, Högstorp H, Wadin K, Rask-Andersen H. 2009. Variational anatomy of the human cochlea: Implications for cochlear implantation. Otology and Neurotology 30(1):14-22.
Escudé B, James C, Deguine O, Cochard N, Eter E, Fraysse B. 2006. The size of the cochlea and predictions of insertion depth angles for cochlear implant electrodes. Audiology and Neurotology 11(Suppl. 1):27-33.
Finley CC, Holden TA, Holden LK, Whiting BR, Chole RA, Neely GJ, Hullar TE, Skinner MW. 2008. Role of electrode placement as a contributor to variability in cochlear implant outcomes. Otology & neurotology : official publication of the American Otological Society, American Neurotology Society [and] European Academy of Otology and Neurotology 29(7):920-928.
Finley CC, Wilson BS, White MW. 1990. Models of neural responsiveness to electrical stimulation. In: Miller JM, Spelman FA, editors. Cochlear Implants. New York: Springer-Verlag Inc. p. 55-96.
Fishman AJ. 2012. Imaging and anatomy for cochlear implants. Otolaryngol Clin North Am 45(1):1-24.
Fredelake S, Hohmann V. 2012. Factors affecting predicted speech intelligibility with cochlear implants in an auditory model for electrical stimulation. Hearing Research 287(1-2):76-90.
Frijns JHM, Briaire JJ, Grote JJ. 2001. The importance of human cochlear anatomy for the results of modiolus-hugging multichannel cochlear implants. Otology and Neurotology 22(3):340-349.
Frijns JHM, Briaire JJ, Schoonhoven R. 2000a. Integrated use of volume conduction and neural models to simulate the response to cochlear implants. Simulation Practice and Theory 8(1-2):75-97.

Frijns JHM, Briaire JJ, Schoonhoven R. 2000b. Integrated use of volume conduction and neural models to simulate the response to cochlear implants. Simulation Practice and Theory 8:75-97.
Frijns JHM, de Snoo SL, Schoonhoven R. 1995. Potential distributions and neural excitation patterns in a rotationally symmetric model of the electrically stimulated cochlea. Hearing Research 87(1–2):170-186.
Frijns JHM, De Snoo SL, Ten Kate JH. 1996. Spatial selectivity in a rotationally symmetric model of the electrically stimulated cochlea. Hearing Research 95(1-2):33-48.
Gantz BJ, Woodworth GG, Knutson JF, Abbas PJ, Tyler RS. 1993. Multivariate predictors of audiological success with multichannel cochlear implants. Annals of Otology, Rhinology and Laryngology 102(12):909-916.
Girzon G. 1987. Investigation of current flow in the inner ear during electrical stimulation of intracochlear electrodes, [Msc]. [Massachusetts Institute of Technology]: Massachusetts Institute of Technology.
Govindasamy R. 2012. Modelling subject-specific electrically evoked auditory neural responses in the guinea pig [Masters dissertation]. [Pretoria]: University of Pretoria.
Greenwood D. 1990. A cochlear frequency-position function for several species - 29 years later. Journal of the Acoustical Society of America 87:2592-2605.
Gstoettner W, Franz P, Hamzavi J, Plenk Jr H, Baumgartner W, Czerny C. 1999. Intracochlear position of cochlear implant electrodes. Acta Otolaryngol 119(2):229-33.
Hanekom T. 2001. Three-dimensional spiraling finite element model of the electrically stimulated cochlea. Ear and Hearing 22(4):300-315.
Hanekom T. 2005. Modelling encapsulation tissue around cochlear implant electrodes. Medical and Biological Engineering and Computing 43(1):47-55.
Hartley DEH, Vongpaisal T, Xu J, Shepherd RK, King AJ, Isaiah A. 2010. Bilateral cochlear implantation in the ferret: A novel animal model for behavioral studies. Journal of Neuroscience Methods 190(2):214-228.
Hartmann R, Klinke R. 1990. Response characteristics of nerve fibres to patterned electrical stimulation. In: Miller JM, Spelman FA, editors. Cochlear implants. Models of the electrically stimulated ear. New York: Springer. p. 135-160.
Hassanzadeh S, Farhadi M, Daneshi A, Emamdjomeh H. 2002. The effects of age on auditory speech perception development in cochlear-implanted prelingually deaf children. Otolaryngology - Head and Neck Surgery 126(5):524-527.
Hatsushika SI, Shepherd RK, Tong YC, Clark GM, Funasaka S. 1990. Dimensions of the scala tympani in the human and cat with reference to cochlear implants. Annals of Otology, Rhinology and Laryngology 99:871-876.
Irving S, Trotter MI, Fallon JB, Millard RE, Shepherd RK, Wise AK. 2013. Cochlear implantation for chronic electrical stimulation in the mouse. Hearing Research 306:37-45.
Isaiah A, Vongpaisal T, King AJ, Hartley DEH. 2014. Multisensory training improves auditory spatial processing following bilateral cochlear implantation. Journal of Neuroscience 34(33):11119-11130.
Jeschke M, Moser T. 2015. Considering optogenetic stimulation for cochlear implants. Hearing Research 322:224-234.
Johnstone BM, Johnstone JR, Pugsley ID. 1966. Membrane resistance in endolymphatic walls of the first turn of the guinea-pig cochlea. Journal of the Acoustical Society of America 40(6):1398-1404.
Kalkman RK, Briaire JJ, Dekker DM, Frijns JHM. 2014a. Place pitch versus electrode location in a realistic computational model of the implanted human cochlea. Hearing Research 315C:10-24.
Kalkman RK, Briaire JJ, Dekker DMT, Frijns JHM. 2014b. Place pitch versus electrode location in a realistic computational model of the implanted human cochlea. Hearing Research 315:10-24.
Kalkman RK, Briaire JJ, Frijns JHM. 2015. Current focussing in cochlear implants: An analysis of neural recruitment in a computational model. Hearing Research 322:89-98.

Kang S, Chwodhury T, Moon IJ, Hong SH, Yang H, Won JH, Woo J. 2015. Effects of electrode position on spatiotemporal auditory nerve fiber responses: A 3D computational model study. Computational and Mathematical Methods in Medicine 2015.

Kendi TK, Arikan OK, Koç C. 2004. Magnetic resonance imaging of cochlear modiolus: determination of mid-modiolar area and modiolar volume. The Journal of Laryngology & Otology 118(7):496-499.

Ketten DR. 1994. The role of temporal bone imaging in cochlear implants. Current Opinion in Otolaryngology & Head and Neck Surgery 2(5):401-408.

Ketten DR, Skinner MW, Wang G, Vannier MW, Gates GA, Neely JG. 1998a. IN VIVO MEASURES OF COCHLEAR LENGTH AND INSERTION DEPTH OF NUCLEUS COCHLEAR IMPLANT ELECTRODE ARRAYS Annals of Otology, Rhinology and Laryngology 175(Suppl):1-16.

Ketten DR, Skinner MW, Wang G, Vannier MW, Gates GA, Neely JG. 1998b. In vivo measures of cochlear length and insertion depth of nucleus cochlear implant electrode arrays. Ann Otol Rhinol Laryngol Suppl 175:1-16.

Kral A, Hartmann R, Mortazavi D, Klinke R. 1998. Spatial resolution of cochlear implants: the electrical field and excitation of auditory afferents. Hearing Research 121:11-28.

Krombach GA, van den Boom M, Di Martino E, Schmitz-Rode T, Westhofen M, Prescher A, Gunther RW, Wildberger JE. 2005. Computed tomography of the inner ear: size of anatomical structures in the normal temporal bone and in the temporal bone of patients with Meniere's disease. Eur Radiol 15(8):1505-13.

Lane JI, Witte RJ, Driscoll CL, Shallop JK, Beatty CW, Primak AN. 2007. Scalar localization of the electrode array after cochlear implantation: clinical experience using 64-slice multidetector computed tomography. Otol Neurotol 28(5):658-62.

Lau H, Ruys AJ, Carter P, Wang X, Li Q. 2011. Subject specific modelling of electrical conduction in the body: A case study. Journal of Biomimetics, Biomaterials, and Tissue Engineering 1314(10):45-53.

Le Breton A, Jegoux F, Pilet P, Godey B. 2015. Micro-CT scan, electron microscopy and optical microscopy study of insertional traumas of cochlear implants. Surgical and Radiologic Anatomy 37(7):815-823.

Lee CF, Li GJ, Wan SY, Lee WJ, Tzen KY, Chen CH, Song YL, Chou YF, Chen YS, Liu TC. 2010. Registration of micro-computed tomography and histological images of the guinea pig cochlea to construct an ear model using an iterative closest point algorithm. Annals of Biomedical Engineering 38(5):1719-27.

Li PMMC, Wang H, Northrop C, Merchant SN, Nadol Jr JB. 2007. Anatomy of the round window and hook region of the cochlea with implications for cochlear implantation and other endocochlear surgical procedures. Otology and Neurotology 28(5):641-648.

Liu B, Gao XL, Yin HX, Luo SQ, Lu J. 2007. A detailed 3D model of the guinea pig cochlea. Brain Structure and Function 212(2):223-230.

Maarefvand M, Marozeau J, Blamey PJ. 2013. A cochlear implant user with exceptional musical hearing ability. International Journal of Audiology 52(6):424-432.

Malherbe TK, Hanekom T, Hanekom JJ. 2013. Can subject-specific single-fibre electrically evoked auditory brainstem response data be predicted from a model? Medical Engineering and Physics 35(7):926-936.

Malherbe TK, Hanekom T, Hanekom JJ. 2015a. Constructing a three-dimensional electrical model of a living cochlear implant user's cochlea. International Journal for Numerical Methods in Biomedical Engineering.

Malherbe TK, Hanekom T, Hanekom JJ. 2015b. The effect of the resistive properties of bone on neural excitation and electric fields in cochlear implant models. Hearing Research 327:126-135.

Martinez-Monedero R, Niparko JK, Aygun N. 2011. Cochlear coiling pattern and orientation differences in cochlear implant candidates. Otology & Neurotology 32(7):1086-1093

Marx M, Risi F, Escude B, Durmo I, James C, Lauwers F, Deguine O, Fraysse B. 2014. Reliability of cone beam computed tomography in scalar localization of the electrode array: a radio histological study. Eur Arch Otorhinolaryngol 271(4):673-9.
Melhem ER, Shakir H, Bakthavachalam S, MacDonald CB, Gira J, Caruthers SD, Jara H. 1998. Inner ear volumetric measurements using high-resolution 3D T2-weighted fast spin-echo MR imaging: initial experience in healthy subjects. American Journal of Neuroradiology 19(10):1819-22.
Micco AG, Richter CP. 2006. Electrical resistivity measurements in the mammalian cochlea after neural degeneration. Laryngoscope 116(8):1334-1341.
Murugasu E, Hans P, Jackson A, Ramsden RT. 1999. The application of three-dimensional magnetic resonance imaging rendering of the inner ear in assessment for cochlear implantation. Am J Otol 20(6):752-7.
Naganawa S, Ito T, Iwayama E, Fukatsu H, Ishigaki T, Nakashima T, Ichinose N. 1999. MR imaging of the cochlear modiolus: Area measurement in healthy subjects and in patients with a large endolymphatic duct and sac. Radiology 213(3):819-823.
National Institute on Deafness and Other Communication Disorders. Science Capsule: Cochlear Implants [Internet]. Available from: http://www.nidcd.nih.gov/about/plans/2012-2016/Pages/Science-Capsule-Cochlear-Implants.aspx
Neri E, Caramella D, Cosottini M, Zampa V, Jackson A, Berrettini S, Sellari-Franceschini S, Bartolozzi C. 2000. High-resolution magnetic resonance and volume rendering of the labyrinth. Eur Radiol 10(1):114-8.
Newbold C, Mergen S, Richardson R, Seligman P, Millard R, Cowan R, Shepherd R. 2014. Impedance changes in chronically implanted and stimulated cochlear implant electrodes. Cochlear Implants International 15(4):191-199.
Nicoletti M, Wirtz C, Hemmert W. 2013. Modeling sound localization with cochlear implants. The technology of binaural listening. Springer. p. 309-331.
Noble JH, Labadie RF, Majdani O, Dawant BM. 2011. Automatic segmentation of intracochlear anatomy in conventional CT. IEEE Transactions on Biomedical Engineering 58(9):2625-2632.
Noble JH, Rutherford RB, Labadie RF, Majdani O, Dawant BM. Modeling and segmentation of intra-cochlear anatomy in conventional CT. 2010.
Nussbaum D, LaPorta R, Hinger J. Cochlear Implants and Sign Language. Sharing Ideas; 11-12 April 2002 2002; Gallaudet University: Laurent Clerc National Deaf Education Center. p. 1-85.
O'Leary SJ, Black RC, Clark GM. 1985. Current distributions in the cat cochlea: A modeling and electrophysiological study. Hearing Research 18:273-281.
Pelliccia P, Venail F, Bonafe A, Makeieff M, Iannetti G, Bartolomeo M, Mondain M. 2014. Cochlea size variability and implications in clinical practice. Acta Otorhinolaryngol Ital 34(1):42-9.
Peters BR, Wyss J, Manrique M. 2010. Worldwide trends in bilateral cochlear implantation. The Laryngoscope 120(5):17-44.
Pfingst BE, Donaldson JA, Miller JM, Spelman FA. 1979. Psychophysical evaluation of cochlear prostheses in a monkey model. Annals of Otology, Rhinology and Laryngology 88(5 I):613-625.
Poznyakovskiy AA, Zahnert T, Kalaidzidis Y, Schmidt R, Fischer B, Baumgart J, Yarin YM. 2008. The creation of geometric three-dimensional models of the inner ear based on micro computer tomography data. Hearing Research 243(1-2):95-104.
Rattay F. 1986. Analysis of models for external stimulation of axons. IEEE Transactions on Biomedical Engineering 33(10):974-977.
Rattay F, Leao RN, Felix H. 2001a. A model of the electrically excited human cochlear neuron. II. Influence of the three-dimensional cochlear structure on neural excitability. Hearing Research 153(1–2):64-79.
Rattay F, Lutter P, Felix H. 2001b. A model of the electrically excited human cochlear neuron: I. Contribution of neural substructures to the generation and propagation of spikes. Hearing Research 153(1–2):43-63.

Rau TS, Hussong A, Herzog A, Majdani O, Lenarz T, Leinung M. 2011. Accuracy of computer-aided geometric 3D reconstruction based on histological serial microgrinding preparation. Computer Methods in Biomechanics and Biomedical Engineering 14(7):581-594.
Rebscher SJ, Hetherington AM, Snyder RL, Leake PA, Bonham BH. 2007. Design and fabrication of multichannel cochlear implants for animal research. Journal of Neuroscience Methods 166(1):1-12.
Reda FA, McRackan TR, Labadie RF, Dawant BM, Noble JH. 2014. Automatic segmentation of intra-cochlear anatomy in post-implantation CT of unilateral cochlear implant recipients. Medical Image Analysis 18(3):605-615.
Rodt T, Ratiu P, Becker H, Bartling S, Kacher DF, Anderson M, Jolesz FA, Kikinis R. 2002. 3D visualisation of the middle ear and adjacent structures using reconstructed multi-slice CT datasets, correlating 3D images and virtual endoscopy to the 2D cross-sectional images. Neuroradiology 44(9):783-790.
Rubinstein JT. 2004. An introduction to the biophysics of the electrically evoked compound action potential. International Journal of Audiology 43(SUPPL. 1):S3-S9.
Samp C. 2010. Cochlear implants in the deaf community: Current circumstances of cochlear implant users among the deaf youth in Sweden's educational system. Rochester Institute of Technology.
Seemann MD, Seemann O, Bonél H, Suckfüll M, Englmeier KH, Naumann A, Allen CM, Reiser MF. 1999. Evaluation of the middle and inner ear structures: Comparison of hybrid rendering, virtual endoscopy and axial 2D source images. European Radiology 9(9):1851-1858.
Seitz J, Held P, Waldeck A, Strotzer M, Volk M, Strutz J, Feuerbach S. 2001. Value of high-resolution MR in patients scheduled for cochlear implantation. Acta Radiol 42(6):568-73.
Shpizner BA, Holliday RA, Roland JT, Cohen NL, Waltzman SB, Shapiro WH. 1995. Postoperative imaging of the multichannel cochlear implant. AJNR Am J Neuroradiol 16(7):1517-24.
Skinner MW, Ketten DR, Holden LK, Harding GW, Smith PG, Gates GA, Neely JG, Kletzker GR, Brunsden B, Blocker B. 2002. CT-Derived Estimation of Cochlear Morphology and Electrode Array Position in Relation to Word Recognition in Nucleus-22 Recipients. JARO - Journal of the Association for Research in Otolaryngology 3(3):332-350.
Skinner MW, Ketten DR, Vannier MW, Gates GA, Yoffie RL, Kalender WA. 1994. Determination of the position of nucleus cochlear implant electrodes in the inner ear. Am J Otol 15(5):644-51.
Sladen DP, Zappler A. 2015. Older and younger adult cochlear implant users: Speech recognition in quiet and noise, quality of life, and music perception. American Journal of Audiology 24(1):31-39.
Snel-Bongers J, Briaire JJ, Van Der Veen EH, Kalkman RK, Frijns JHM. 2013. Threshold levels of dual electrode stimulation in cochlear implants. JARO - Journal of the Association for Research in Otolaryngology 14(5):781-790.
Sobrinho FP, Lazarini PR, Yoo HJ, Abreu Júnior L, de Sá Meira A. 2009. A method for measuring the length of the cochlea through magnetic resonance imaging. Brazilian journal of otorhinolaryngology 75(2):261-267.
Spelman FA, Clopton BM, Pfingst BE. 1982. Tissue impedance and current flow in the implanted ear. Implications for the cochlear prosthesis. Annals of Otology, Rhinology and Laryngology Supplement (United States) 91(Suppl 98):3-8.
Stakhovskaya O, Sridhar D, Bonham BH, Leake PA. 2007. Frequency map for the human cochlear spiral ganglion: Implications for cochlear implants. JARO - Journal of the Association for Research in Otolaryngology 8(2):220-233.
Strelioff D. 1973a. A computer simulation of the generation and distribution of cochlear potentials. Journal of the Acoustical Society of America 54(3):620-629.
Strelioff D. 1973b. A computer simulation of the generation and distribution of cochlear potentials. The Journal of the Acoustical Society of America 54(3):620-629.
Strydom T, Hanekom JJ. 2011. An analysis of the effects of electrical field interaction with an acoustic model of cochlear implants. Journal of the Acoustical Society of America 129(4):2213-2226.

Taha T, Wahba H, Ibrahim AS, AbdElazim Y. 2015. Cochlear implant tailored imaging protocol: What clinicians need to know. The Egyptian Journal of Radiology and Nuclear Medicine 46(1):33-43.
Teymouri J, Hullar TE, Holden TA, Chole RA. 2011. Verification of computed tomographic estimates of cochlear implant array position: a micro-CT and histologic analysis. Otol Neurotol 32(6):980-6.
Tran P, Sue A, Wong P, Li Q, Carter P. 2014. Development of HEATHER for cochlear implant stimulation using a new modeling workflow. IEEE Transactions on Biomedical Engineering 62(2):728-735.
Vaid S, Vaid N. 2014. Imaging for cochlear implantation: structuring a clinically relevant report. Clin Radiol 69(7):e9-e24.
van der Marel KS, Briaire JJ, Wolterbeek R, Snel-Bongers J, Verbist BM, Frijns JH. 2014. Diversity in cochlear morphology and its influence on cochlear implant electrode position. Ear Hear 35(1):e9-20.
van Wermeskerken GK, Prokop M, van Olphen AF, Albers FW. 2007. Intracochlear assessment of electrode position after cochlear implant surgery by means of multislice computer tomography. Eur Arch Otorhinolaryngol 264(12):1405-7.
Vanpoucke F, Zarowski A, Casselman J, Frijns J, Peeters S. 2004a. The facial nerve canal: An important cochlear conduction path revealed by clarion electrical field imaging. Otology and Neurotology 25(3):282-289.
Vanpoucke F, Zarowski A, Peeters S. 2004b. Identification of the impedance model of an implanted cochlear prosthesis from intracochlear potential measurements. IEEE Transactions on Biomedical Engineering 51(12):2174-2183.
Verbist BM, Ferrarini L, Briaire JJ, Zarowski A, dmiraal-Behloul F, Olofsen H, Reiber JHC, Frijns JHM. 2009. Anatomic considerations of cochlear morphology and its implications for insertion trauma in cochlear implant surgery. Otology and Neurotology 30(4):471-477.
Verbist BM, Joemai RM, Briaire JJ, Teeuwisse WM, Veldkamp WJ, Frijns JH. 2010a. Cochlear coordinates in regard to cochlear implantation: a clinically individually applicable 3 dimensional CT-based method. Otol Neurotol 31(5):738-44.
Verbist BM, Joemai RMS, Teeuwisse WM, Veldkamp WJH, Geleijns J, Frijns JHM. 2008. Evaluation of 4 multisection CT systems in postoperative imaging of a cochlear implant: A human cadaver and phantom study. American Journal of Neuroradiology 29(7):1382-1388.
Verbist BM, Skinner MW, Cohen LT, Leake PA, James C, Boex C, Holden TA, Finley CC, Roland PS, Roland JT, Jr. et al. . 2010b. Consensus panel on a cochlear coordinate system applicable in histologic, physiologic, and radiologic studies of the human cochlea. Otol Neurotol 31(5):722-30.
Vermeire K, Landsberger DM, Van de Heyning PH, Voormolen M, Kleine Punte A, Schatzer R, Zierhofer C. 2015. Frequency-place map for electrical stimulation in cochlear implants: Change over time. Hearing Research 326:8-14.
Voie AH, Burns DH, Spelman FA. 1993. Orthogonal-plane fluorescence optical sectioning: Three-dimensional imaging of macroscopic biological specimens. Journal of Microscopy 170(3):229-236.
Voie AH, Spelman FA. 1995. Three-dimensional reconstruction of the cochlea from two-dimensional images of optical sections. Computerized Medical Imaging and Graphics 19(5):377-384.
von Békésy G. 1951. The coarse pattern of the electrical resistance in the cochlea of the guinea pig (Electroanatomy of the cochlea). The Journal of the Acoustical Society of America 23(1):18-28.
Wada H, Sugawara M, Kobayashi T, Hozawa K, Takasaka T. 1998. Measurement of guinea pig basilar membrane using computer-aided three- dimensional reconstruction system. Hearing Research 120(1-2):1-6.
Wang G, Vannier MW. 1998. Spiral CT image deblurring for cochlear implantation. IEEE Transactions on Medical Imaging 17(2):251-262.

Wang H, Northrop C, Burgess B, Liberman MC, Merchant SN. 2006. Three-dimensional virtual model of the human temporal bone: A stand-alone, downloadable teaching tool. Otology and Neurotology 27(4):452-457.
Westen AA, Dekker DM, Briaire JJ, Frijns JH. 2011. Stimulus level effects on neural excitation and eCAP amplitude. Hear Res 280(1-2):166-76.
Whiten DM. 2007. Electro-anatomical models of the cochlear implant. [Cambridge, Massachusetts, USA]: Massachusetts Institute of Technology. p. 225.
Whiting BR, Holden TA, Brunsden BS, Finley CC, Skinner MW. 2008. Use of computed tomography scans for cochlear implants. Journal of Digital Imaging 21(3):323-328.
Won JH, Jones GL, Moon IJ, Rubinstein JT. 2015. Spectral and temporal analysis of simulated dead regions in cochlear implants. JARO - Journal of the Association for Research in Otolaryngology 16(2):285-307.
Wong P, George S, Tran P, Sue A, Carter P, Li Q. 2016. Development and Validation of a High Fidelity Finite Element Model of Monopolar Stimulation in the Implanted Guinea Pig Cochlea. Biomedical Engineering, IEEE Transactions on 63(1):188-198.
Wong P, Sue A, Tran P, Inguva C, Li Q, Carter P. 2015. Time-domain simulation of volume conduction in the guinea pig cochlea. Conference on Implantable Auditory Prostheses (CIAP). Granlibakken, Lake Tahoe, USA: Association for Research in Otolaryngology (ARO). p. 217.
Wurfel W, Lanfermann H, Lenarz T, Majdani O. 2014. Cochlear length determination using Cone Beam Computed Tomography in a clinical setting. Hear Res 316:65-72.
Xu Y, Collins LM. 2004. Predicting the threshold of pulse-train electrical stimuli using a stochastic auditory nerve model: the effects of stimulus noise. Biomedical Engineering, IEEE Transactions on 51(4):590-603.
Yoo KS, Wang G, Rubinstein JT, Skinner MW, Vannier MW. 2000a. Three-dimensional modeling and visualization of the cochlea on the internet. IEEE Transactions on Information Technology in Biomedicine 4(2):144-151.
Yoo SK, Wang G, Collison F, Rubinstein JT, Vannier MW, Kim HJ, Kim NH. 2004. Three-Dimensional Localization of Cochlear Implant Electrodes Using Epipolar Stereophotogrammetry. IEEE Transactions on Biomedical Engineering 51(5):838-846.
Yoo SK, Wang G, Rubinstein JT, Vannier MW. 2000b. Three-dimensional geometric modeling of the cochlea using helico-spiral approximation. IEEE Transactions on Biomedical Engineering 47(10):1392-1402.
Zaidman-Zait A. 2010. Quality of life among cochlear implant recipients. In: Stone JH, Blouin M, editors. International Encyclopedia of Rehabilitation Buffalo, NY: Center for International Rehabilitation Research Information and Exchange (CIRRIE).
Zeng FG, Rebscher S, Harrison W, Sun X, Feng H. 2008. Cochlear implants: system design, integration, and evaluation. IEEE reviews in biomedical engineering 1:115-142.
Zhang X, Gan RZ. 2011. A comprehensive model of human ear for analysis of implantable hearing devices. IEEE Transactions on Biomedical Engineering 58(10 PART 2):3024-3027.
Zhaol T, Hongxia Y, Shuqian L. Visualization of guinea pig cochlea by computed tomography of diffracttion enhanced imaging. Complex Medical Engineering, 2007. CME 2007. IEEE/ICME International Conference on; 23-27 May 2007 2007. p. 994-997.
Zou J, Hannula M, Lehto K, Feng H, Lahelma J, Aula AS, Hyttinen J, Pyykko I. 2015. X-ray microtomographic confirmation of the reliability of CBCT in identifying the scalar location of cochlear implant electrode after round window insertion. Hear Res 326:59-65.